Constraints on Nitrogen Cycling at the Subtropical North Pacific Station ALOHA from Isotopic Measurements of Nitrate and Particulate Nitrogen.

K. L. Casciotti[1], T. W. Trull[2], D. M. Glover[1], and D. Davies[2].

1. Department of Marine Chemistry and Geochemistry, Woods Hole Oceanographic Institution, Woods Hole, MA 02543.

2. Antarctic Climate and Ecosystems Cooperative Research Center, University of Tasmania, and Commonwealth Scientific and Industrial Research Organization, Marine and Atmospheric Research, Hobart, Australia.

Abstract

Nitrogen supply to surface waters can play an important role in the productivity and ecology of subtropical ecosystems. As part of the Vertical Transport in the Global Ocean (VERTIGO) program, we examined the fluxes of nitrogen to and from the euphotic zone at station ALOHA in the north Pacific subtropical gyre using natural abundance stable isotopic measurements of nitrate ($\delta^{15}N_{NO3}$ and $\delta^{18}O_{NO3}$), as well as sinking and suspended particulate nitrogen ($\delta^{15}N_{PN}$). Paralleling the steep gradient in nitrate concentration in the upper thermocline at ALOHA, we observed a steep gradient in $\delta^{15}N_{NO3}$, decreasing from a maximum of +7.1‰ at 500 meters (m) to +1.5-2.4‰ at 150 m. $\delta^{18}O_{NO3}$ values also decreased from +3.0 ‰ at 300 m to +0.7-0.9 ‰ at 150 m. The decreases in both $\delta^{15}N_{NO3}$ and $\delta^{18}O_{NO3}$ require inputs of isotopically "light" nitrate to balance the upward flux of nitrate with high $\delta^{15}N_{NO3}$ (and $\delta^{18}O_{NO3}$). We conclude that both nitrogen fixation and diagenetic alteration of the sinking flux contribute to the decrease in $\delta^{15}N_{NO3}$ and $\delta^{18}O_{NO3}$ in the upper thermocline at station ALOHA. While nitrogen

fixation is required to explain the nitrogen isotope patterns, the rates of nitrogen fixation may be lower than previously estimated. By including high-resolution nitrate isotope measurements in the nitrogen isotope budget for the euphotic zone at ALOHA, we estimate that approximately 25%, rather than 50%, of export production was fueled by N_2 fixation during our study. On the other hand, this input of N_2-derived production accumulates in the upper thermocline over time, playing a significant role in subtropical nutrient cycling through maintenance of the subsurface nitrate pool. An increase in sinking $\delta^{15}N_{PN}$ between 150-300 m, also suggests that fractionation during remineralization contributed to the low $\delta^{15}N_{NO3}$ values observed in this depth range by introducing a subsurface nitrate source that is 0.5 ‰ lower in $\delta^{15}N$ than the particle flux exported from the euphotic zone. While the time scale of these observations are currently limited, they highlight the need for inclusion of $\delta^{15}N_{NO3}$ measurements in a time series program to allow a broader assessment of the variations in subsurface $\delta^{15}N_{NO3}$ values and the links between subsurface nitrate and export flux at station ALOHA.

1. Introduction

Station ALOHA nitrogen cycling and export

Station ALOHA is home to one of the longest running oceanographic time series observational programs and much is known about the seasonal dynamics and interannual variability of physical and biogeochemical processes at this site, as well as the long-term trends in physical, chemical, and biological properties (Dore et al., 2002; Karl, 1999; Karl et al., 2001a; Karl et al., 1995). As a representative of one of the earth's largest biomes (Karl et al., in press), it is important to understand what limits primary production and export in this oligotrophic environment. The nitracline at ALOHA is positioned at 110 ± 10 m (Dore and Karl, 1996). These depths are within the euphotic zone, but at or below the limit of maximum winter mixed layer depths (Dore et al., 2002; Fennel et al., 2002). It has been argued, therefore, that nitrate supply to the mixed layer is limited to mesoscale eddy activity and infrequent event-driven pulses or vertical migration of phytoplankton (Karl, 1999; Letelier et al., 2000; Sakamoto et al., 2004; Vaillancourt et al., 2003; Villareal et al., 1993; Villareal et al., 1996). This part of the oligotrophic north Pacific subtropical gyre also relies on nitrogen fixation as a source of nitrogen for primary production, particularly in the mixed layer or upper euphotic zone (Dore et al., 2002; Karl et al., 1997; Mahaffey et al., 2005). However, productivity in the lower euphotic zone may be largely nitrate-driven (Fennel et al., 2002; Letelier et al., 2004). Of the average 0.8-1 mol C m^{-2} y^{-1} exported from the surface ocean at the Hawaii Ocean Time Series station ALOHA approximately 48%, or 0.4-0.5 mol C m^{-2} y^{-1}, has been attributed to nitrogen fixation (Karl et al., 1997).

Independent lines of evidence at station ALOHA have highlighted the quantitative importance of N fixation as a mode of new production in the north Pacific subtropical gyre. High

abundance (Church et al., 2005a; Letelier and Karl, 1996) and diversity (Falcon et al., 2004; Zehr et al., 1998; Zehr et al., 2001) of diazotrophic cyanobacteria, as well as tight physical associations between nitrogen fixing cyanobacteria and eukaryotic phytoplankton (Karl et al., 1997; Scharek et al., 1999), illustrate the capacity for nitrogen fixation. In addition, the activity of diazotrophic phytoplankton has been measured through short-term incubation experiments (Dore et al., 2002; Montoya et al., 2004; Zehr et al., 2001) and expression of genes coding for nitrogenase (Zehr et al., 2001; Church et al., 2005b). In addition to instantaneous measurements, the role of nitrogen fixation in seasonal and annual export production has been inferred through nitrogen stable isotopic budgets (Dore et al., 2002; Karl et al., 1997) and geochemical modeling of gas ratios and nutrient stoichiometry (Karl et al., 1997; Fennel et al., 2002; Deutsch et al., 2007; Emerson et al., 1995). The results of these studies highlight the potential importance of N fixation as a mode of new production in the north Pacific subtropical gyre.

If the euphotic zone is neither gaining nor losing nitrogen, the export of particulate nitrogen (PN) from the surface ocean should be balanced by supplies of new nitrogen through nitrate input, nitrogen fixation, and atmospheric deposition. Moreover, if steady state can be assumed on an annual timescale, then the nitrogen isotopic content ($\delta^{15}N$ ‰ = $[((^{15}N/^{14}N)_{sample}/(^{15}N/^{14}N)_{std}) -1] *1000$) of the incoming and outgoing nitrogen fluxes should also balance. While long-term changes in the nutrient inventories have been observed at ALOHA (Karl et al., 1997; Karl et al., 2001a; Karl et al., 2001b), the time scale for this change is long relative to the fluxes through the system. A nitrogen isotope balance approach has been taken by Karl et al (1997) and Dore et al (2002) to estimate that the fraction of annual export production supported by nitrogen fixation at ALOHA averages about 48%, with a seasonal pattern that indicates a higher fraction of export supported by N_2 fixation in the summer when waters are

strongly stratified, and a lower fraction of export supported by N_2 fixation in the winter when mixed layers extend down to 100 m.

The construction of isotope budgets to infer annual rates of N_2 fixation at ALOHA relied on sparse measurements of nitrate $\delta^{15}N$ ($\delta^{15}N_{NO3}$) in the north Pacific (Liu et al., 1996; Voss et al., 2001), but none at or near station ALOHA. Based on these measurements, the supply of nitrate to the surface water at ALOHA has been assumed to possess a $\delta^{15}N$ value of +6.5‰ (Dore et al., 2002). As noted by Mahaffey et al (2005) if the $\delta^{15}N$ of nitrate sources to the euphotic zone at ALOHA are less than 6.5‰, the N input from N_2 fixation may be less than currently estimated from long-term measurements of sinking $\delta^{15}N_{PN}$ values. Since that time, a few $\delta^{15}N_{NO3}$ measurements have been reported from station ALOHA (Mahaffey et al., in press; Sutka et al., 2004), but these data were not used to confirm or refute this assumed isotopic value for nitrate entering the euphotic zone at station ALOHA. Indeed, because of the strong gradients in the water column, high spatial resolution nitrate isotopic data are required for this assessment, and thus to determine the accuracy of isotope-based fluxes of new and export production and the integrated contribution of nitrogen fixation to subsurface nitrate at this site. These fluxes have important implications for understanding the mechanisms of carbon export from the north Pacific subtropical gyre and the physical and ecological constraints on new production in the oligotrophic ocean.

As part of the Vertical Transport in the Global Ocean (VERTIGO) program, we occupied station ALOHA for a three-week period from June 20 to July 11, 2004. This cruise occurred immediately following HOT 160 (June 14-18, 2004) and preceding HOT 161 (July 12-14, 2004). During the VERTIGO cruise many physical, chemical, and biological parameters were measured repeatedly over the three-week period, including primary productivity, new and regenerated

106 production, particle export and attenuation through the mesopelagic zone (Buesseler et al., this
107 issue). These measurements were designed to capture the surface properties related to particle
108 flux measured at nominal depths of 150, 300, and 500 m, as well as to examine the mechanisms
109 controlling particle flux attenuation. During this expedition, observations of particle export flux
110 (Buesseler et al., 2007), were similar to the low levels historically observed in July and August at
111 station ALOHA (Christian et al., 1997; Dore et al., 2002; Karl et al., 1996). Although the particle
112 fluxes are low at this oligotrophic site, mesopelagic particle attenuation at ALOHA is very
113 efficient, with 20% or less of the carbon flux at 150 m passing 500 m (Buesseler et al., 2007). If
114 remineralization drives this flux attenuation, or at least keeps pace with it, this could represent a
115 significant flux of nitrogen into the subsurface, accumulating as nitrate.
116 The current study was undertaken to examine the nitrogen cycling and supply to the
117 euphotic zone at station ALOHA using high-resolution $\delta^{15}N_{NO3}$ and $\delta^{18}O_{NO3}$ measurements in
118 the context of the study of particle flux dynamics offered by the VERTIGO program.
119 Measurements of nitrate $\delta^{15}N$ and $\delta^{18}O$ ($\delta^{18}O$ ‰ = $[((^{18}O/^{16}O)_{sample}/(^{18}O/^{16}O)_{std}) - 1] * 1000$), as
120 well as sinking and suspended particulate nitrogen $\delta^{15}N$, were made through the upper
121 mesopelagic (150-500 m) where the bulk of particulate export is remineralized. We relate the
122 isotopic distributions in nitrate and particulate nitrogen to uptake and remineralization of
123 nitrogen in the upper water column. These results allow us to assess the influence of nitrogen
124 fixation and particle remineralization on the accumulation of nitrate in the upper thermocline.
125

2. Methods

2.1 Sample collection

All samples reported here were collected within 18 nautical miles of station ALOHA (22º 45' N, 158º W) in the North Pacific Subtropical Gyre during June 20 – July 11 2004. Over the three-week period, samples were collected for $\delta^{15}N_{NO3}$ and $\delta^{18}O_{NO3}$ measurements from 11 profiles, ranging from depths of 150 m to 3,000 m. Samples were collected from 10 L Niskin bottles into 60 mL HDPE Nalgene bottles, rinsed three times with sample before final volumes were collected. Samples were frozen immediately on board, transported frozen, and stored at –20 ºC until isotopic analysis.

Suspended particles were collected from the Multiple Unit Large Volume Filtration System (MULVFS; Bishop et al., 1985) at depths of 30, 54, 79, 104, 153, 202, 326, 474, 572, and 770 m. Particles were collected from 3,840 to 12,790 L of seawater (J. Bishop, personal communication), depending on the depth, by filtering in-situ over a four hour period through a 53 μm nylon mesh and then two layers of (pre-combusted) QMA quartz fiber filter (1 μm nominal pore size). The MULVFS QMA filters were subsampled upon retrieval in a HEPA-filtered laminar flow hood by excising 47 mm discs, which were then frozen.

Sinking particles were collected in replicate Neutrally-Buoyant Sediment Traps (NBST's; Buesseler et al., 2000; Valdes and Price, 2000) deployed at nominal depths of 150 m (3 traps), 300 m (2 traps), and 500 m (2 traps). The traps were each deployed for two 3-5 day collections during the cruise. Each trap held five replicate tubes containing 500 mL brine (freeze-condensed filtered Sargasso seawater) poisoned with 180 μM $HgCl_2$ or 2% formalin (Buesseler et al., 2007; Lamborg et al., this issue; Lee et al., 1992). The brine (with particles) from the replicate tubes were combined, pre-screened through 350-μm mesh to remove "swimmers", and split into 8

149 equal volumes on board after recovery of the traps (Lamborg et al., this issue). Sample splits for
150 $\delta^{15}N_{PN}$ measurements from the first set of NBST trap deployments at ALOHA were filtered onto
151 pre-combusted 25 mm silver filters, dried, and stored frozen until analysis. Only $HgCl_2$-treated
152 samples were analyzed here for $\delta^{15}N_{PN}$.
153
154 *2.2 Nitrate isotopic analysis*
155 Nitrate (plus nitrite) $\delta^{15}N$ and $\delta^{18}O$ analyses were performed using the denitrifier method,
156 as previously described (Casciotti et al., 2002; Sigman et al., 2001). Based on nitrate (plus
157 nitrite) concentration analyses, sample volumes were calculated to achieve either 5 nmoles
158 (samples from 150-200 m) or 20 nmoles (samples from >200 m) for a given batch of analyses.
159 At either target sample size, aliquots of nitrate isotopic reference materials USGS32, USGS34,
160 and USGS35 (Böhlke et al., 2003) were analyzed in parallel, with an aliquot of each standard
161 analyzed after every 9 samples. The matching of sample and standard amounts simplifies the
162 isotopic calibration of sample analyses based on parallel analyses of standards. The use of
163 USGS32, USGS34, and USGS35 provides a 2-3 point calibration curve for $\delta^{15}N_{NO3}$ and $\delta^{18}O_{NO3}$
164 measurements. Calibration to the most recently reported $\delta^{15}N$ and $\delta^{18}O$ values for these materials
165 (Böhlke et al., 2003) yields $\delta^{15}N_{NO3}$ values of 5.5‰ and $\delta^{18}O_{NO3}$ values of 1.6-2.0‰ for the deep
166 (>3000 m) Pacific (this study; Casciotti, unpublished data). The $\delta^{18}O_{NO3}$ values are therefore
167 higher in comparison to previous results (e.g. Casciotti et al., 2002; Sigman et al., 2005).
168 Average $\delta^{15}N_{NO3}$ and $\delta^{18}O_{NO3}$ values and standard deviations reported here are based on replicate
169 analyses (n=2-4) of each sample, with analyses conducted on multiple days representing
170 independent batches of bacteria and standard calibrations. $\delta^{15}N_{NO3}$ values are reported in permil
171 (‰) vs. AIR and $\delta^{18}O_{NO3}$ values are reported in permil (‰) vs. VSMOW.

Nitrite was not removed from these samples or analyzed separately for isotopic composition. Based on historical data for station ALOHA, nitrite was expected to be less than 100 nmol kg^{-1} at 150 m and lower than 20 nmol kg^{-1} at 200 m and below (Dore and Karl, 1996). At 150 m, then, nitrite may have been as much as 20% of the combined nitrate and nitrite pools, but at concentrations of 100 nmol kg^{-1} or less, nitrite is not isotopically accessible. To achieve pure $\delta^{15}N_{NO3}$ and $\delta^{18}O_{NO3}$ values, these samples would need to be treated with ascorbic acid to remove nitrite (Granger et al., 2006). However, the combined nitrate plus nitrite pool is relevant for discussion of the euphotic zone nitrogen mass balance.

2.3 Particulate nitrogen $\delta^{15}N$ analysis

Frozen MULVFS subsamples were thawed, then dried at 60 °C. Once dried, ten to twenty punches (5 mm each) from the top QMA filter were combined to achieve approximately 5 μg N for $\delta^{15}N_{PN}$ analyses. From splits of sinking material, whole 25 mm filters were used, which contained approximately 2-20 μg N per filter. In either case, filters were packed into silver capsules, treated with 1N HCl to remove carbonates, and dried overnight at 60°C. The capsules were then crimped shut and analyzed using a Fisions 1500 Elemental Analyzer and ConFlo-II interface inline with a Finnigan Delta^{PLUS} isotope ratio mass spectrometer. A small-bore combustion tube (Karsh et al., 2003) was also used to increase sensitivity (signal amplitude) for the small quantities of sinking and suspended material collected in this study. Individual analyses were normalized to N_2 working gases and to AIR reference scales by parallel analyses of IAEA-N1 (ammonium sulfate, $\delta^{15}N$ = +0.4‰) and IAEA-N3 (potassium nitrate, $\delta^{15}N$ = +4.7‰). Precision for $\delta^{15}N$ standard analyses was 0.11‰ and 0.12‰ during runs for suspended and sinking $\delta^{15}N_{PN}$, respectively.

3. Results

3.1 Physical properties

The water column at station ALOHA is stably stratified with mixed layer depths ranging seasonally from 40 m in the summer to 80-100 m in the winter (Dore et al., 2002; Fennel et al., 2002). Below the surface mixed layer, five water masses have been identified: Subtropical Salinity Maximum Water (STSMW; σ_θ = 24.2 kg m^{-3}, centered at ~150 m), Shallow Salinity Minimum Water (SSMW; σ_θ = 25.8 kg m^{-3}, centered at ~300 m), North Pacific Intermediate Water (NPIW; σ_θ = 26.8 kg m^{-3}, centered at ~500 m), North Pacific Deep Water (NPDW; σ_θ = 27.5 kg m^{-3}, ~1000 m), and North Pacific Bottom Water (σ_θ = 27.8 kg m^{-3}, below 3000 m) (Sabine et al., 1995; Talley, 1985; Talley, 1993). Temperature, salinity, and density data are shown in Figure 1A, with data from HOT 160 shown as smoothed curves and data from VERTIGO corresponding to nitrate isotope samples represented by the circles. Because the primary focus of this study was to place constraints on the fluxes and isotopic dynamics of nitrate supply and remineralization in the "twilight" zone, the majority of samples for $\delta^{15}N_{NO3}$ and $\delta^{18}O_{NO3}$ analyses were collected from the upper water column (150-600 m), consisting of SSTMW, SSMW, and NPIW. Samples collected from NPBW and NPDW were intended for intercomparison to other measurements taken from the north Pacific basin (Liu and Kaplan, 1989; Liu et al., 1996; Sigman et al., 2005; Voss et al., 2001). Waters above 150 m were sampled but did not contain sufficient nitrate for isotopic analyses.

3.2 Nutrient distributions

The nutrient fields in HOT cruises 160 and 161 (immediately preceding and immediately after the VERTIGO cruise, respectively) were nearly identical to each other, with nanomolal nitrate concentrations in the euphotic zone, increasing to a maximum of 41 μmol kg^{-1} at 700-1000 m. The nutrient measurements made in the VERTIGO program were similar to HOT data in the upper 500 m (where the majority of VERTIGO sampling was conducted), but showed greater divergence from historical ALOHA data in deeper waters (data not shown). Because we were interested in full depth profiles for the current study, VERTIGO nitrate concentration data were not used here. Instead, nitrate data obtained from the HOT-DOGS data server (http://hahana.soest.hawaii.edu/hot/hot-dogs/interface.html) for HOT cruises 160 and 161 were used to determine the profile of nitrate concentrations (μmol kg^{-1}) at depths sampled for $\delta^{15}N_{NO3}$ and $\delta^{18}O_{NO3}$. Where necessary, available data were interpolated linearly between HOT standard depths to obtain nitrate concentrations at the appropriate depths. Figure 1B displays nitrate, phosphate, and oxygen concentration data from HOT 160 (lines) and interpolated nitrate and phosphate concentration values for the depths at which VERTIGO nitrate isotope samples were collected (circles). The interpolated nitrate concentrations obtained in this way matched well with the nitrate concentrations estimated from integrated ion beam amplitudes during the nitrate isotopic analyses. Nitrate concentrations ranged from approximately 0.2-0.5 μmol kg^{-1} at 150 m to a maximum of 41 μmol kg^{-1} in the oxygen minimum at 700-1000 m.

3.3 Nitrate $\delta^{15}N$ and $\delta^{18}O$

Paralleling the steep decrease in nitrate concentration from 500 to 150 m, we found a steep decrease in $\delta^{15}N_{NO3}$ from 7.0-7.1 ‰ (average +7.1 ± 0.2‰) at 500 m to 1.5-2.4‰ (average +1.9 ± 0.3‰) at 150 m (Figure 2A). The steep decrease in $\delta^{15}N_{NO3}$ in the upper thermocline has

been observed in other tropical and subtropical locations (Karl et al., 2002; Knapp et al., 2005; Liu et al., 1996) and is consistent with recent results from station ALOHA (Mahaffey et al., in press; Sutka et al., 2004). In waters below 500 m, $\delta^{15}N_{NO3}$ gradually decreased to 5.4 ± 0.2‰, which is typical for deep water in the north Pacific (Brandes et al., 1998; Cline and Kaplan, 1975; Liu et al., 1996; Sigman et al., 2005; Sutka et al., 2004).The potential mechanisms driving the observed distribution in $\delta^{15}N_{NO3}$ at ALOHA, in particular the upward decrease in $\delta^{15}N_{NO3}$ between 500 and 150 m, are evaluated below.

$\delta^{18}O_{NO3}$ also decreased in the upper thermocline, from maximum values of +2.5 to +3.3‰ (average +3.0 ± 0.2‰) at 300 m to values of +0.7 to +1.0 (average +0.9 ± 0.3‰) at 150 m (Figure 2A). Such low $\delta^{18}O_{NO3}$ values have not previously been reported in near-surface waters and would likely represent an upper limit on the $\delta^{18}O_{NO3}$ of freshly produced oceanic nitrate. Between 500 m and 300 m, where $\delta^{15}N_{NO3}$ shows a decreasing trend, $\delta^{18}O_{NO3}$ continues to increase above its 500 m value, causing the maximum in $\delta^{18}O_{NO3}$ to be shallower than the maximum in $\delta^{15}N_{NO3}$ (Figure 2A). Offsets in the depths of $\delta^{15}N_{NO3}$ and $\delta^{18}O_{NO3}$ maxima have been observed in other regions, such as in waters overlying the oxygen deficient zone in the eastern tropical north Pacific (Sigman et al., 2005), where it was interpreted to result from remineralization of newly fixed nitrogen or subsurface nitrate/nitrite recycling. The mechanisms driving the relative changes in $\delta^{15}N_{NO3}$ and $\delta^{18}O_{NO3}$ at ALOHA will be discussed in more detail below. $\delta^{18}O_{NO3}$ continued to decrease below 500 m to a value of +1.6 ± 0.3‰ at 3047 m. This $\delta^{18}O_{NO3}$ value is higher than previously reported deep Pacific values (+0.3‰, Casciotti et al., 2002; -0.5‰, Sigman et al., 2005) but less than expected from the offset in calibration schemes (2.9‰) for $\delta^{18}O_{NO3}$ with previous work (see the Methods section).

263 *3.3 Suspended/sinking $\delta^{15}N$-PN*

264 The $\delta^{15}N$ of suspended particles (suspended $\delta^{15}N_{PN}$) also increased with depth from
265 +2.8‰ at 153 m to +6.7‰ at 326 m, then decreased steadily to +6.0‰ at 770 m (Figure 2B).
266 Values as low as +0.5 to +0.8‰ were observed in the mixed layer (30-50 m). These data are
267 consistent with observations from HOT 160 during which suspended $\delta^{15}N_{PN}$ measurements
268 ranged from –0.3‰ at 43 m to +2.2‰ at 175 m. Low suspended $\delta^{15}N_{PN}$ have also been observed
269 in other tropical and subtropical surface waters. In the Sargasso Sea, for example, suspended
270 $\delta^{15}N_{PN}$ values are in the range of –1.0 to +2.0‰ (Altabet, 1988; Altabet et al., 1991; Montoya et
271 al., 2002). Variations in suspended $\delta^{15}N_{PN}$ can reflect numerous factors, including $\delta^{15}N$ of new
272 nitrogen sources (N_2, NO_3^-), fractionation during assimilation, as well as recycled phytoplankton
273 production fueled by excretion of ammonium by zooplankton, and trophic complexity (Altabet,
274 1988; Trull et al., in press). At station ALOHA, little DIN accumulates in the euphotic zone so
275 fractionation during DIN assimilation is not likely to be expressed in suspended $\delta^{15}N_{PN}$.
276 However, zooplankton activity (Al-Mutairi and Landry, 2001; Landry et al., 2001; Steinberg et
277 al., this issue) may help to preferentially retain low $\delta^{15}N$ material in the surface waters (Altabet,
278 1988; Checkley and Miller, 1989; Montoya et al., 2002).

279 Sinking $\delta^{15}N_{PN}$ is more diagnostic of the sources of new N to the euphotic zone (N_2 or
280 NO_3^-) than suspended $\delta^{15}N_{PN}$ because its flux should balance the mass and isotope fluxes of new
281 nitrogen at steady state (Altabet, 1988; Lourey et al., 2003; Knapp et al., 2005). We measured
282 sinking $\delta^{15}N_{PN}$ of +2.3 to +2.8‰ (average +2.5 ± 0.4‰) at 150 m, +3.3 to +3.6‰ (average +3.5
283 ± 0.2‰) at 300 m and +3.1 to +3.6‰ (average +3.3 ± 0.3‰) at 500 m (Figure 2B). The results
284 from the 150 m traps are comparable to results from the HOT program that show sinking $\delta^{15}N_{PN}$
285 at 150 m ranging seasonally from –1 to +7‰ (Dore et al., 2002), with sinking $\delta^{15}N_{PN}$ values of

286 +3.0 ± 0.9‰ in June, +3.1 ± 0.8‰ in July, and +2.6 ± 1.0‰ in August averaged over the
287 available HOT dataset from 1989-2006 (http://hahana.soest.hawaii.edu/hot/hot-
288 dogs/interface.html). In 2004, summer sinking $\delta^{15}N_{PN}$ from the HOT dataset was consistent at
289 3.1‰ from July (HOT 160) and +3.05‰ in August (HOT 162).
290
291 **4. Discussion**
292 *4.1 N isotope budget for ALOHA*
293 Sources of new nitrogen to the surface ocean can be analyzed using isotope budgets for
294 nitrogen sources and sinks from the euphotic zone. If the surface ocean is neither gaining nor
295 losing nitrogen, both mass and isotopic composition of the incoming and outgoing fluxes should
296 balance when integrated over a sufficiently long time period. Conceptually, the mass balance is
297 based on a two-component mixing model where the fluxes of new nitrogen (F_{N2} and F_{NO3}) and
298 their isotopic composition ($\delta^{15}N_{N2fix}$ and $\delta^{15}N_{NO3}$, respectively) are combined to produce the flux
299 of sinking PN (F_{PN}) with isotopic composition ($\delta^{15}N_{PN}$): $\delta^{15}N_{N2fix} \times F_{N2} + \delta^{15}N_{NO3} \times F_{NO3} =$
300 $\delta^{15}N_{PN} \times F_{PN}$. This two-component model has been used at many sites (e.g. Altabet, 1988;
301 Francois et al., 1992; Liu et al., 1996), including station ALOHA (e.g. Dore et al., 2002; Karl et
302 al., 1997) to estimate the proportion of annual nitrogen export that is driven by nitrogen fixation
303 and that driven by nitrate assimilation. In the absence of $\delta^{15}N_{NO3}$ data from station ALOHA, the
304 $\delta^{15}N$ contribution from nitrate was assumed to be +6.5‰, as measured previously in north
305 Pacific deep water (Wada and Hattori, 1990), and the $\delta^{15}N$ contribution from newly fixed N was
306 assumed to be 0‰. From annual average sinking $\delta^{15}N_{PN}$, these calculations have suggested that
307 nitrogen fixation supplies approximately 48% of new nitrogen to the euphotic zone at station
308 ALOHA on an annual basis (Dore et al., 2002; Karl et al., 1997).

Based on the high-resolution $\delta^{15}N_{NO3}$ data reported here, this approach can now be further refined. It is observed that the $\delta^{15}N_{NO3}$ of the upwardly diffusing nitrate flux is modified as it transits from deep waters to the point of assimilation in the euphotic zone above 150 m, and our data suggest that nitrate crossing into the euphotic zone at station ALOHA at 150 m has a $\delta^{15}N_{NO3}$ significantly lower than +6.5‰ in June and July of 2004. The $\delta^{15}N_{NO3}$ value taken to represent the upward nitrate flux, however, depends on the assumed mechanism of nitrate supply to surface waters. If steady-state diffusion is assumed to dominate the upward flux of nitrate, the $\delta^{15}N_{NO3}$ flux can be calculated from vertical gradients in concentration of ^{15}N and ^{14}N in nitrate: $\delta^{15}N_{NO3} = (d[^{15}N_{NO3}]/dz \div d[^{14}N_{NO3}]/dz) \div {}^{15}R_{std} - 1)*1000$, where $^{15}R_{std}$ is the $^{15}N/^{14}N$ ratio of air. Taking gradients in $[^{15}N_{NO3}]$ and $[^{14}N_{NO3}]$ over 150-250 m and over 150-300 m results in upward flux $\delta^{15}N_{NO3}$ values of +3.0‰ or +3.7‰, respectively. If, instead, nitrate is assumed to enter the euphotic zone primarily through sporadic injections fueled by mesoscale eddy activity, the $\delta^{15}N_{NO3}$ flux might be represented by the depth integral of $[^{15}N_{NO3}]$ and $[^{14}N_{NO3}]$ over the depth range from which nutrients are injected, i.e. +2.5‰ for 150-200 m, +3.5‰ for 150-250 m, or +4.5‰ for 150-300 m. Uncertainty in the relative importance of these mechanisms for nitrate supply to the euphotic zone, leads to ranges in the estimated $\delta^{15}N_{NO3}$ flux of +3.0 to +3.7‰ (diffusion) or +2.5 to +4.5‰ (injection). At the same time, the downward flux of sinking PN at 150 m had a measured $\delta^{15}N_{PN}$ of 2.5 ± 0.4‰. Incorporating these values into the two-component mixing model and propagating errors for each component leads to estimates of 0-44% (average of estimates: 24 ± 19%) of exported N supplied by N_2 fixation in summer 2004 if $\delta^{15}N_{N2fix}$ is taken to be 0 ± 1‰ (Dore et al., 2002 and references therein), or 0-37% (average of estimates: 19 ± 16%) if $\delta^{15}N_{N2fix}$ is taken to be –1 ± 1‰ (Brandes and Devol, 2002 and references therein; Liu et al., 1996; Minagawa and Wada, 1986). These flux proportions are much lower than previous

estimates for N_2-derived export at ALOHA and suggest that the mass flux of N from fixation in the euphotic zone contributed approximately 25% of the sinking PN flux captured at 150 m during VERTIGO (0.25 × 0.18 mmol N m^{-2} d^{-1} or 0.045 mmol N m^{-2} d^{-1}). This implied N_2 fixation rate is also much less than rates previously estimated at ALOHA based on annual average sinking $\delta^{15}N_{PN}$ (Karl et al., 1997).

Of course, our calculations are based on measurements spanning only three weeks in summer of 2004 and do not represent an annual budget. We assume for the purposes of this study that fluxes of nitrogen into and out of the euphotic zone are balanced over the time period of our measurements. This is supported by data from the HOT program that suggest that the PN fluxes were not changing substantially in magnitude or in $\delta^{15}N$ over the summer of 2004 (http://hahana.soest.hawaii.edu/hot/hot-dogs/interface.html). For example, the sinking PN fluxes at 150 m from HOT 160 (June) and HOT 162 (August) were 0.39 mmol m^{-2} d^{-1} and 0.21 mmol m^{-2} d^{-1}, respectively compared with our 0.18 mmol m^{-2} d^{-1}; furthermore, sinking $\delta^{15}N_{PN}$ at 150 m was 3.11‰ and 3.05‰ during HOT 160 and 162, respectively, compared with our +2.5‰. Bottom-moored sediment traps at HALE-ALOHA also did not show significant changes in export flux for several months prior to our occupation of station ALOHA (Buesseler et al., this issue). Therefore, we argue that the sinking flux measured during VERTIGO was within the range of summer flux measurements from station ALOHA measured during the HOT program and most likely did not reflect a response to recent disturbance. Higher sinking $\delta^{15}N_{PN}$ values observed at other times of year in the HOT record may indicate access of nitrate from deeper in the water column or non-steady state behavior where nitrate is upwelled and exported in pulses that allow the nitrate-N to be increased in $\delta^{15}N$ above the values observed here (Mahaffey et al., in press). However, in the context of prior observations at ALOHA, nitrogen fixation is expected

to be highest in summertime, and the sinking $\delta^{15}N_{PN}$ that we measure is consistent with previous estimates (Dore et al., 2002). The main difference is the lower $\delta^{15}N$ estimated for the nitrate end member in this study.

Remineralization of DON has also been neglected in this study. If newly fixed nitrogen is exported as DON from the euphotic zone or transported laterally away from this site, we could be missing this contribution to the mass and isotope balances. Thus far, the available data suggests that horizontal gradients of DON in the vicinity of ALOHA are weak, although vertical gradients could support a small flux of DON out of the euphotic zone (Abell et al., 2000). However, the limited data available on $\delta^{15}N$ of high molecular weight DON ($\delta^{15}N_{DON}$) at ALOHA (Mahaffey et al., 2005; Meador et al., 2007) suggests that it is not a reservoir of low $\delta^{15}N$ material.

4.2 Sources of low $\delta^{15}N$ nitrate: mixing, remineralization, recycling

The $\delta^{15}N_{NO3}$ values at station ALOHA decrease from a maximum $\delta^{15}N_{NO3}$ at 500 m to a minimum $\delta^{15}N_{NO3}$ at 150 m. This large decrease in $\delta^{15}N_{NO3}$ occurs in spite of simultaneously decreasing nitrate concentrations. Nitrate consumption in the sunlit surface waters maintains nitrate concentrations at exceedingly low levels in the upper 150 m, and accordingly any residual nitrate should be highly enriched in ^{15}N relative to the supplies of nitrate (local nitrification or advection/diffusion from below). Mixing of this residual nitrate pool with nitrate diffusing up from below would be expected to generate a $\delta^{15}N_{NO3}$ profile that is upwardly increasing, if only slightly due to the low residual nitrate concentration (Figure 3; Knapp et al., 2005; Casciotti et al., 2002; Sigman et al., 1999). In order to generate an upwardly decreasing trend in $\delta^{15}N_{NO3}$, a

source of low $\delta^{15}N_{NO3}$ is needed to offset the upward flux of high $\delta^{15}N_{NO3}$ and the removal of low $\delta^{15}N_{NO3}$ during assimilation.

Trends of decreasing $\delta^{15}N_{NO3}$ towards the surface have been observed in other tropical and subtropical sites (Figure 3; Karl et al., 2002; Knapp et al., 2005; Liu et al., 1996). The low $\delta^{15}N_{NO3}$ values at these sites may result from nitrogen fixation, providing a source of low $\delta^{15}N_{PN}$ for remineralization, from zooplankton excretion of low $\delta^{15}N_{NH4}$ that is then oxidized to nitrate, or from preferential remineralization of low $\delta^{15}N$-fractions from particulate nitrogen (Altabet, 1988; Lehmann et al., 2002). In the Kuroshio region of the western subtropical Pacific, Liu et al (1996) reported subsurface (100-300 m) $\delta^{15}N_{NO3}$ values as low as –0.5‰ at one site, although average $\delta^{15}N_{NO3}$ values in this depth range were +3.3 ± 0.4‰. $\delta^{15}N_{NO3}$ values increased above this isotopic minimum to +4.6 ± 0.9‰ in surface waters; below the isotopic minimum, $\delta^{15}N_{NO3}$ values gradually increased to average deep Pacific values of 5‰ (Liu et al., 1996). Based on an analysis of the nitrogen isotope budget, it was argued that the euphotic zone nitrogen isotope budget was roughly balanced with nitrate supply ($\delta^{15}N_{NO3}$ = +3.3‰) and PN export ($\delta^{15}N_{PN}$ = 3.5‰), requiring little nitrogen fixation to balance the budget on an annual basis (8% of annual export). However, the subsurface nitrate pool showed the influence of nitrogen fixation in the lowered thermocline $\delta^{15}N_{NO3}$ values. They concluded that while nitrogen fixation could account for only a minor amount of new production in Kuroshio surface waters on an annual basis, it was cumulatively responsible for up to 40% of nitrate in subsurface waters, the renewal of which occurs on a much longer time scale. Thus, taking a broader view, N_2 fixation plays an important role in maintaining the subsurface pool of nitrate in this region.

In thermocline waters of the Sargasso Sea, low ^{15}N content is seen in both nitrate (Figure 3; Karl et al., 2002; Knapp et al., 2005) and suspended particulate nitrogen pools (Altabet, 1988;

400 Mahaffey et al., 2003; Montoya et al., 2002). It has been argued that sinking $\delta^{15}N_{PN}$ leaving the
401 euphotic zone in the Sargasso Sea can be approximately balanced by the nitrate supply and does
402 not require significant nitrogen fixation for isotope balance (Altabet, 1988; Knapp et al., 2005).
403 As discussed above, we observed low sinking $\delta^{15}N_{PN}$ (+2.5 ± 0.4‰) and a corresponding
404 flux of low $\delta^{15}N_{NO3}$ (+2.5 to +4.5‰) back into the euphotic zone at ALOHA. The question of
405 why $\delta^{15}N_{NO3}$ values are low in the first place will be addressed here. In the following discussion,
406 two depth ranges will be considered: 1) STSMW-SSMW (150-300 m), and 2) SSMW-NPIW
407 (300-500 m). These depth ranges represent intervals between defined water masses, which may
408 serve as end members for diapycnal mixing.
409
410 *4.2.1 Mixing*
411 The processes contributing to the distribution of $\delta^{15}N_{NO3}$ in the 150-300 m depth range
412 include mixing and remineralization of organic nitrogen (particulate and dissolved). Nitrate will
413 tend to diffuse upward due to its concentration gradient from below 300 m and exit into the
414 euphotic zone above 150 m. These two fluxes are countered by nitrate from remineralization of
415 organic nitrogen coupled to nitrification. Conservative mixing of nitrate between STSMW (150
416 m) and SSMW (300 m) would generate waters with nitrate concentrations and salinities falling
417 along the solid line in Figure 4A. The nitrate concentrations from this depth range fall roughly
418 along the conservative mixing line indicating that sources are roughly balanced by sinks, with
419 perhaps a small net source of nitrate between 150 and 300 m depth. Thus, nitrate in this depth
420 range appears to be roughly in steady-state. However, the non-conservative nature of nitrate in
421 the 150-300 m range is apparent from examination of the $\delta^{15}N_{NO3}$ data. The expected $\delta^{15}N_{NO3}$ vs.
422 salinity trajectory for mixing of STSMW ($[NO_3^-]$ of 0.2 μmol kg^{-1} and average $\delta^{15}N_{NO3}$ of 1.9‰)

423 with SSMW ([NO_3^-] of 9 μmol kg^{-1} and average $\delta^{15}N_{NO3}$ of 5.8‰) is indicated by the solid line
424 in Figure 4B. The steepness of the mixing curve reflects the dominance of the isotopic
425 composition of the mixture by the end member with the higher nitrate concentration (SSMW).
426 The measured $\delta^{15}N_{NO3}$ values fall below this mixing line, indicating the non-conservative nature
427 of $\delta^{15}N_{NO3}$, which requires a source of low $\delta^{15}N_{NO3}$ in the depth range between 150 and 300 m.
428 In deeper waters, the nitrate concentrations suggest a small net sink of nitrate between
429 SSMW (300 m) and NPIW (500 m) (Figure 4A). This could be explained by isopycnal mixing
430 with denitrifying waters in the eastern tropical Pacific (26.7 kg m^{-3}). Maximal $\delta^{15}N_{NO3}$ values at
431 this depth are also consistent with an impact from nitrate removal in remote denitrifying waters.
432 A few $\delta^{15}N_{NO3}$ values from this depth range fall below the mixing line between SSMW (300 m)
433 and NPIW (500 m) (Figure 4B), consistent with a small input of low $\delta^{15}N_{NO3}$, which will be
434 discussed in more detail below.
435 Given that mixing in the 150-300 m and 300-500 m intervals cannot explain the origin of
436 the low $\delta^{15}N_{NO3}$ values, we turn to remineralization of organic nitrogen as a mechanism for
437 lowering $\delta^{15}N_{NO3}$ and examine two potential (and not mutually exclusive) mechanisms for
438 generating the low $\delta^{15}N_{NO3}$ values observed in near surface waters at ALOHA: 1) fractionation
439 due to preferential remineralization of a ^{15}N-depleted fraction of sinking particles, and 2) long-
440 term accumulation of nitrate sourced from N_2-based export in the upper thermocline.
441
442 *4.2.2 Sinking particle remineralization*
443 Particle flux attenuation in the water column can be modeled approximately by a power
444 law $F_z = F_{150}(z/150)^{-b}$, where F_z is the measured flux at a given depth (z) and F_{150} is the measured
445 flux at 150 m. The exponent "b" is derived from an empirical fit to the flux data and dictates the

steepness of the flux attenuation profile (Martin et al., 1987). Averaging both deployments of the NBST sediment traps during the VERTIGO occupation of station ALOHA, the measured flux of organic nitrogen was approximately 0.18 mmol N m^{-2} d^{-1} at 150 m, 0.07 mmol N m^{-2} d^{-1} at 300 m, and 0.03 mmol N m^{-2} d^{-1} at 500 m using NBST sediment traps (Lamborg et al., this issue). These fluxes imply that the coefficient "b" in the flux equation is approximately 1.48 ± 0.12 (C. Lamborg, personal communication), which is similar to that estimated previously from HOT time series data (1.12 ± 0.015; Christian et al., 1997). Based on these measurements of particle flux attenuation, we can also estimate that the remineralization flux is 0.12 mmol N m^{-2} d^{-1} between 150 and 300 m and 0.03 mmol N m^{-2} d^{-1} between 300 and 500 m (Figure 5), assuming solubilization keeps pace with particle disaggregation (i.e. the suspended particle pool is not changing with time).

In addition to nitrogen fixation, isotopic fractionation during particle remineralization may cause preferential retention of low-$\delta^{15}N$ material in the upper water column. Preferential remineralization of a low $\delta^{15}N$ fraction of sinking PN should result in an increase in sinking $\delta^{15}N_{PN}$ with depth. Individual measurements of the $\delta^{15}N$ of sinking particulate nitrogen (sinking $\delta^{15}N_{PN}$) captured in the NBST traps ranged from an average of 2.5 ± 0.4‰ at 150 m to 3.5 ± 0.2‰ at 300 m and 3.3 ± 0.3‰ at 500 m (Figure 2B). The increase in sinking $\delta^{15}N_{PN}$ between 150 and 300 m suggests that fractionation of the particulate N takes place during remineralization in this depth range. From the increase in sinking $\delta^{15}N_{PN}$ between 150 and 300 m seen at ALOHA, we can estimate using mass balance that the nitrate produced from particle remineralization between 150 and 300 m would correspond to a flux of about 0.12 mmol N m^{-2} d^{-1} with a $\delta^{15}N_{NO3}$ of 1.9 ± 0.6‰ (Figure 5). Using a Rayleigh-type model to estimate the isotope effect for this remineralization flux (ε_{remin}) yields 1.0‰, given by $\varepsilon_{remin} = (\delta^{15}N_{PN,150} -$

469 $\delta^{15}N_{PN,300})/(\ln f)$, where f (here having a value of 0.36) is the fraction of particle flux remaining at
470 300 m. The increase in sinking $\delta^{15}N_{PN}$ with depth could be due to preferential remineralization of
471 low $\delta^{15}N$ organic matter in specific classes of organic nitrogen or particle types (Lehmann et al.,
472 2002), although regardless of mechanism, the result is the release of low $\delta^{15}N$ material from the
473 sinking particle flux into the water column between 150 and 300 m. Remineralization of DON
474 may also contribute to the cycling of N in the upper thermocline (Abell et al., 2000; Knapp et al.,
475 2005; Mahaffey et al., 2005). However, $\delta^{15}N_{DON}$ values from ALOHA surface waters (+5.5‰;
476 Mahaffey et al., 2005; Meador et al., 2007) suggest that downward mixing of DON from the
477 euphotic zone and subsequent remineralization may not be a source of low $\delta^{15}N$ material to the
478 thermocline unless there is preferential remineralization of a low-$\delta^{15}N$ component (Knapp et al.,
479 2005).

480 Between 300 and 500 m, the sinking $\delta^{15}N_{PN}$ does not change significantly, but further
481 particle remineralization is expected to contribute 0.03 mmol N m^{-2} d^{-1} of nitrate with $\delta^{15}N_{NO3}$ of
482 approximately 3.7± 0.8‰ (Figure 5). Given that the particle flux and associated remineralization
483 flux decrease with depth, and the nitrate concentration increases with depth, the isotopic impact
484 of the remineralization flux will be greatest in shallow waters. Thus, overall, the production of
485 lowered $\delta^{15}N_{NO3}$ during particle remineralization can contribute to a distribution of $\delta^{15}N_{NO3}$ that
486 decreases towards the surface. However, the particle flux cannot explain all of the observations
487 and an additional source of low $\delta^{15}N_{NO3}$ is required to balance the isotope budget in the 0-300 m
488 and 0-500 m depth ranges.

489 To illustrate this point, one needs only to expand the box over which mass balance is
490 considered from 0-150 m to 0-300 m. Whereas in the 0-150 m nitrogen isotope budget, little
491 nitrogen fixation was required to make up the isotopic difference between upward nitrate flux

492 ($\delta^{15}N_{NO3}$ = +2.5 to +4.5‰) and sinking particle flux ($\delta^{15}N_{PN}$ = +2.5‰), the diffusive nitrate flux
493 at 300 m is estimated to have $\delta^{15}N_{NO3}$ of +6.8‰ and sinking $\delta^{15}N_{PN}$ at 300 m is +3.5‰ (Figure
494 5). Therefore, considering a two-component mixture (NO_3^- and N_2) for nitrogen entering the 0-
495 300 m box, nitrogen fixation is estimated to supply approximately 50% of the nitrogen escaping
496 the 300 m depth horizon. Similarly, if one extends the depth interval for mass balance to 500 m,
497 nitrogen inputs from nitrogen fixation (approximately 54%) are required to balance the diffusive
498 nitrate flux with $\delta^{15}N_{NO3}$ of +7.1‰ and sinking $\delta^{15}N_{PN}$ of +3.3‰ (Figure 5). The large
499 contribution of nitrogen fixation to the sinking PN flux at 300 and 500 m can be reconciled with
500 the low percentage of nitrogen fixation required for isotope balance in the 0-150 m depth range
501 (~25%) by considering the time scale of nitrogen cycling through the upper 300 or 500 m and the
502 vertical distribution of nitrogen sources.
503 The arguments above based on nitrogen isotope balance in the upper 150 m suggests that
504 the instantaneous PN flux is fueled primarily by nitrate uptake, although nitrogen fixation is
505 required to lower the sinking $\delta^{15}N_{PN}$ relative to the nitrate supply. Nitrate averaged over the 150-
506 300 m depth range turns over in approximately 20 years with respect to export. During this time,
507 the remineralized input from nitrogen fixation can accumulate to cause a proportionately greater
508 impact on the $\delta^{15}N_{NO3}$ of the near surface nitrate pool than the isotopically enriched nitrate
509 diffusing up from below. Therefore, in an integrative sense, nitrogen fixation contributes even
510 more significantly to new production in that it enhances the pool of nitrate that diffuses upward
511 to fuel export production. These estimates are consistent with the mass balance models of Liu
512 and coworkers (1996) that showed a large integrated contribution of N_2 fixation to the subsurface
513 nitrate pool despite low annual N estimated fluxes of export due to new nitrogen fixation in the
514 western tropical Pacific.

This mass balance presented in this study (Figure 5) is based on $\delta^{15}N_{NO3}$ and $\delta^{15}N_{PN}$ measurements collected over a three-week period, and studies carried out over the long time series at ALOHA show a large amount of annual and interannual variation in productivity and export (Karl et al., 1996). Stochastic event-driven nutrient injections can also be important drivers of primary production at this site (Letelier et al., 2000; Sakamoto et al., 2004). Given the steep gradient in $\delta^{15}N_{NO3}$ between 150 and 300 m, these events may bring nitrate to the surface with higher $\delta^{15}N$ values, driving export of PN with a higher $\delta^{15}N$. In fact, annual average $\delta^{15}N_{PN}$ values ranging from +2.03 to -+4.15‰ (Dore et al., 2002) suggest that nitrate from below 150 m may be accessed by primary producers on an annual basis. Furthermore, since the turnover time of nitrate at 150 m is on the order of a year with respect to production and consumption fluxes, time series observations may reveal important variations in $\delta^{15}N_{NO3}$ gradients below150 m that might cause the $\delta^{15}N_{NO3}$ of the nitrate flux into the euphotic zone to vary with season. In order to construct a truly annual budget for ^{15}N at station ALOHA, time series measurements of $\delta^{15}N_{NO3}$ are needed to compare with exported $\delta^{15}N_{PN}$ measurements.

4.3 Constraints from $\delta^{18}O_{NO3}$

The depth distribution of $\delta^{18}O_{NO3}$ did not completely track changes in $\delta^{15}N_{NO3}$, with maximum $\delta^{18}O_{NO3}$ values occurring shallower than maximum $\delta^{15}N_{NO3}$ values (Figure 2A). Differences in the depth distributions of $\delta^{15}N_{NO3}$ and $\delta^{18}O_{NO3}$ have been analyzed in previous studies using a nitrate isotope anomaly, defined as $\Delta(15,18)$ (‰) = $(\delta^{15}N_{NO3} - \delta^{15}N_{NO3deep}) - {}^{15}\varepsilon/{}^{18}\varepsilon*(\delta^{18}O_{NO3} - \delta^{18}O_{NO3deep})$ (Sigman et al., 2005), where $\delta^{15}N_{NO3deep}$ and $\delta^{18}O_{NO3deep}$ are the isotopic values of deep ocean nitrate and ${}^{15}\varepsilon/{}^{18}\varepsilon$ is the ratio of isotope effects for $\delta^{15}N_{NO3}$ and $\delta^{18}O_{NO3}$ fractionation, respectively. Studies to date suggest that ${}^{15}\varepsilon/{}^{18}\varepsilon$ is very close to 1 for

538 processes that consume nitrate, such as assimilation (Casciotti et al., 2002; Granger et al., 2004)
539 and denitrification (Granger et al., 2006). Therefore, the anomaly is interpreted to arise from
540 processes involved with nitrate regeneration, such as remineralization of organic matter with low
541 $\delta^{15}N_{NO3}$ (e.g. from nitrogen fixation) (Sigman et al., 2005), reoxidation of nitrite produced from
542 nitrate reduction in the subsurface (Sigman et al., 2005; Casciotti and McIlvin, 2007), or from
543 cycles of incomplete nitrate assimilation and regeneration in surface waters (Sigman et al., 2005;
544 Wankel et al., 2007). As discussed in section 4.2 on the basis of $\delta^{15}N_{NO3}$, nitrogen fixation is
545 likely to have both direct and indirect impacts on the distribution of $\delta^{15}N_{NO3}$ in the upper 300 m
546 at station ALOHA. Below 300 m, communication with denitrifying waters in the eastern tropical
547 Pacific may influence nitrate concentrations (Deutsch et al., 2001) and isotopic values. In this
548 section we focus on the Δ(15,18) trends in the upper 300 m and examine whether the $\delta^{18}O_{NO3}$
549 patterns are consistent with conclusions based on $\delta^{15}N_{NO3}$ and what additional information the
550 $\delta^{18}O_{NO3}$ measurements brings to the interpretation.

551 For the purposes of this study, $\delta^{15}N_{NO3deep}$ and $\delta^{18}O_{NO3deep}$ have been assumed to be
552 +5.4‰ and +1.6‰, respectively, based on our NPBW data (Figure 2A). At station ALOHA,
553 Δ(15,18) decreases steadily between the depth of the NPIW (500 m), through SSMW (300 m), to
554 a minimum of –3.2‰ in the STSMW (150 m) (Figure 6). To first order, the distribution of
555 Δ(15,18) between 150 and 500 m is consistent with the remineralization of low $\delta^{15}N$ organic
556 matter from N_2 fixation and diagenetic fractionation of ^{15}N as discussed above. However, to
557 better understand the mechanisms behind the distribution of Δ(15,18) in the water column at
558 ALOHA, it is instructive to examine the trends of $\delta^{15}N_{NO3}$ and $\delta^{18}O_{NO3}$ on an isotope-isotope
559 plot (Figure 7).

As discussed above, nitrate diffusing upwards across the 300 m depth horizon is mixed with nitrate produced by remineralization coupled to nitrification in the 150-300 m depth range. In addition to lowering $\delta^{15}N_{NO3}$, this process also lowers $\delta^{18}O_{NO3}$, though to a lesser extent. While the input of nitrate from remineralization causes a non-linear mixing curve in $\delta^{15}N_{NO3}$ vs. salinity between SSMW (300 m) and STSMW (150 m) (Figure 4B), it generates a straight mixing line between the two end members (SSMW and remineralization flux) on an isotope-isotope plot (Figure 7, dashed arrow). Our observations suggest that this mixing line has a slope of 0.59 ± 0.03. The remineralization flux therefore has the tendency to lower $\delta^{15}N_{NO3}$ more than it lowers $\delta^{18}O_{NO3}$, causing shallow nitrate to extend further from the 1:1 line that serves as the basis of the definition for Δ(15,18). Increasing amounts of remineralization thus lead to a more negative Δ(15,18) signal, with the minimum in Δ(15,18) corresponding to waters in which all of the nitrate originates from the remineralization flux. In order to calculate Δ(15,18) values for the 150 m samples, it is necessary to extend the 1:1 line below the deep water $\delta^{15}N_{NO3}$ and $\delta^{18}O_{NO3}$ values (Figure 7, dotted line). This extension is largely hypothetical because data are only expected to fall along this extension of the 1:1 line under very special circumstances where the remineralization end member happens to fall along the 1:1 line below the $\delta^{15}N_{NO3deep}$ and $\delta^{18}O_{NO3deep}$ values.

The $\delta^{15}N_{NO3}$ of the remineralization end member is controlled by the $\delta^{15}N_{PN}$ that is remineralized (and the isotope effect that is expressed during remineralization). The $\delta^{18}O_{NO3}$ value of the remineralization end member is set by the process of nitrification. The $\delta^{18}O_{NO3}$ signature for oceanic nitrification is not well understood at this time, but our data put an upper limit on the $\delta^{18}O$ of nitrate produced by nitrification in this region. If we take the average $\delta^{15}N_{NO3}$ and $\delta^{18}O_{NO3}$ values measured at 150 m to represent the remineralization flux, this yields

583 a $\delta^{15}N_{NO3}$ of +1.9 ± 0.3‰ and $\delta^{18}O_{NO3}$ of +0.9 ± 0.3‰. The $\delta^{15}N_{NO3}$ of the remineralization flux
584 estimated in this way is indistinguishable from the $\delta^{15}N_{NO3}$ of the remineralization flux estimated
585 from mass and isotope balance of the sinking PN, or +1.9 ± 0.6‰ (Figure 5). The $\delta^{18}O_{NO3}$ is
586 similar, though slightly higher than the commonly accepted $\delta^{18}O_{NO3}$ value of 0‰ for nitrification
587 (Casciotti et al., 2002; Sigman et al., 2005; Wankel et al., 2007; Casciotti and McIlvin, 2007).
588 The $\delta^{15}N_{NO3}$ and $\delta^{18}O_{NO3}$ values from 150 m may overestimate the $\delta^{15}N_{NO3}$ and $\delta^{18}O_{NO3}$ values
589 for nitrification, given that nitrate assimilation may be impacting the shallowest portion of this
590 depth range (raising $\delta^{15}N_{NO3}$ and $\delta^{18}O_{NO3}$ above the source value), and that nitrate with higher
591 $\delta^{15}N_{NO3}$ and $\delta^{18}O_{NO3}$ is diffusing up from below.

592 The $\delta^{15}N_{NO3}$ of the remineralization flux could be lower if dissolved organic nitrogen
593 (DON) or suspended PN with a $\delta^{15}N$ value lower than 2‰ is remineralized in the 150-300 m
594 range. $\delta^{15}N$ values as low as +1.5 ± 1.5‰ have been reported for high molecular weight DON
595 (HMW DON) from cultures of *Trichodesmium* (Meador et al., 2007), although the same study
596 reported $\delta^{15}N$ values for bulk HMW DON at ALOHA of 5.5‰. If the nitrogen undergoing
597 remineralization does have a $\delta^{15}N$ less than 2‰ on average, this would push the estimates (along
598 the dashed arrow in Figure 7) of the $\delta^{18}O_{NO3}$ of the nitrification end member to values closer to
599 0‰. If the previous $\delta^{18}O_{NO3}$ estimates of ~0 ‰ are appropriate for nitrification, the value
600 inferred for the $\delta^{15}N_{NO3}$ of the nitrogen undergoing remineralization would be 0.66 ± 0.24‰.

601 Based on the current dataset we can estimate that the $\delta^{18}O_{NO3}$ of the nitrification source is
602 likely to be between 0 and 0.9‰. We interpret the gradual decrease in both $\delta^{15}N_{NO3}$ and $\delta^{18}O_{NO3}$
603 towards the surface to result from remineralization adding nitrate with low $\delta^{15}N_{NO3}$ and $\delta^{18}O_{NO3}$
604 values relative to deep nitrate. At the same time, this remineralization flux causes Δ(15,18) to
605 decrease due to the fact that the mixing line between 300 m and the remineralization source has a

606 slope that is less than 1. This leads to progressively decreasing Δ(15,18) values in shallow
607 waters, where the remineralization flux has greater influence relative to upward diffusion of deep
608 nitrate (Figure 5).

609 From NPBW (3000 m) to NPDW (1000 m), both $\delta^{15}N_{NO3}$ and $\delta^{18}O_{NO3}$ increase (Figure 7;
610 solid arrow). This is likely a result of communication of these waters with the eastern tropical
611 Pacific where denitrification fractionates both $\delta^{15}N_{NO3}$ and $\delta^{18}O_{NO3}$ with a large isotope effect
612 (Sigman et al., 2005; Casciotti and McIlvin, 2007). Between NPIW and SSMW (300 m), $\delta^{15}N_{NO3}$
613 decreases while $\delta^{18}O_{NO3}$ continues to increase. Similar subsurface trends in $\delta^{15}N_{NO3}$ and $\delta^{18}O_{NO3}$
614 have been attributed to remineralization of newly fixed N (Sigman et al., 2005; Casciotti and
615 McIlvin, 2007) and nitrate/nitrite cycling (Sigman et al., 2005; Casciotti and McIlvin, 2007) but
616 these studies focused on an oceanographic setting with a demonstrable subsurface nitrate sink
617 through denitrification. Given the available data, we cannot confidently propose a mechanism for
618 the coupled changes in $\delta^{15}N_{NO3}$ and $\delta^{18}O_{NO3}$ between 300 and 500 m. However, we note that that
619 waters at 300 m (SSMW) and waters at 500 m (NPIW) have different source properties and
620 circulation histories (Talley, 1985; Talley, 1993), with SSMW originating in the northeast
621 Pacific and NPIW originating in the northwest Pacific, which could lead to different processes
622 affecting these water masses and their trajectories in Δ(15,18) space. Consideration of lateral
623 isopycnal transport using a 2-dimensional dataset may be required to explain the isotopic
624 distributions in the subsurface, but this is beyond the scope of the current study.
625
626 *5. Conclusions: Significance for estimates of N_2 fixation at ALOHA*
627 Previous studies have used isotope mass balance mixing models to estimate the
628 proportion of annual nitrogen export that is driven by nitrogen fixation and that driven by nitrate

assimilation (Dore et al., 2002; Karl et al., 1997). Using available data, the $\delta^{15}N$ contribution from newly fixed N was assumed to be 0‰ and the $\delta^{15}N$ contribution from nitrate was assumed to be +6.5‰. Our new high-resolution nitrate isotope data suggest that the source of nitrate to surface waters in June/July 2004 is considerably lower, in the range of +2.5 to +4.5‰. These values in turn imply a contribution from nitrogen fixation to the export of nitrogen from the euphotic zone at station ALOHA of 25% or less during the VERTIGO study period. Our sinking $\delta^{15}N_{PN}$ values are within the range of summer sinking $\delta^{15}N_{PN}$ values previously reported from ALOHA, which have been interpreted to reflect a large amount of nitrogen fixation (~ 50% of export production) occurring in summer months (Dore et al., 2002). The major difference in our study is the refinement of the estimate of the $\delta^{15}N_{NO3}$ end member. Moreover, our measurements have the potential to reveal links between the supply of new nitrogen, export, and subsurface remineralization processes. In addition to reflecting variable intensities of the two sources of new nitrogen, sinking $\delta^{15}N_{PN}$ may also reflect variations in the $\delta^{15}N_{NO3}$ of nitrate utilized in the euphotic zone or the depth from which nitrate is drawn. Of course, our measurements were limited to a single period in a single summer, and time series measurements of $\delta^{15}N_{NO3}$ are needed to fully understand the potential seasonal and interannual variability in the $\delta^{15}N$ of the nitrate source to the euphotic zone.

The contribution of N_2 fixation to nitrogen export is one factor that causes low $\delta^{15}N_{PN}$ values at this site. In addition, once the low $\delta^{15}N_{PN}$ is exported below 150 m the increase in sinking $\delta^{15}N_{PN}$ between 150 and 300 m suggests that it is remineralized with an isotope effect that preferentially traps ^{14}N in the upper water column and exports ^{15}N (a process that is revealed in our $\delta^{18}O_{NO3}$ data, which are the first for this site). The combination of these two processes cause the accumulated nitrate in the upper thermocline to retain a much larger isotopic signal

652 from N_2 fixation than from upwelled deep nitrate. The vertical distribution of these processes
653 generates an upwardly decreasing trend in $\delta^{15}N_{NO3}$ towards the surface and supplies low $\delta^{15}N_{NO3}$
654 to the euphotic zone, which serves to further lower sinking $\delta^{15}N_{PN}$. Thus, we find that at steady
655 state, organic N produced from N_2 fixation contributes both directly and indirectly to the export
656 flux, with exported N_2-fixer biomass remineralized into nitrate in the upper mesopelagic playing
657 an important role in sustaining export production.

Figure Legends

Figure 1: (A) Depth profiles of temperature, salinity, and density at station ALOHA. Data from VERTIGO are indicated by circles and data from HOT 160 are shown as lines for each property. (B) Depth profiles of nitrate, phosphate, and oxygen at station ALOHA. Data from HOT 160 are shown as lines, and interpolated nitrate and phosphate data at the depths of VERTIGO nitrate isotope samples are indicated by circles.

Figure 2: (A) Depth profiles of $\delta^{15}N_{NO3}$ (filled circles) and $\delta^{18}O_{NO3}$ (open circles) at station ALOHA. Error bars indicate ±1 standard deviation of replicate measurements (n=2-4) for each sample. (B) Depth profiles of suspended $\delta^{15}N_{PN}$ (filled diamonds) and sinking $\delta^{15}N_{PN}$ (open squares) at station ALOHA during VERTIGO (June/July 2004). Error bars represent ±1 standard deviation of replicate analyses of standard materials at the time of sample analyses.

Figure 3: Comparison of ALOHA depth profiles of $\delta^{15}N_{NO3}$ with previous results: ALOHA (this study; filled circles), western tropical Pacific (Liu and Kaplan, 1996; open circles), Bermuda Atlantic Time Series station (Knapp et al., 2005; filled diamonds), Sargasso Sea (Karl et al., 2002; open diamonds), and Subarctic Pacific (Casciotti et al., 2002; dot-dashed line).

Figure 4: (A) Property-property plot of VERTIGO [NO_3^-] vs. salinity results. Symbol sizes correspond to sample depths and associated water masses, and lines indicate conservative mixing between STSMW (150 m) and SSMW (300 m) (solid line), SSMW and NPIW (500 m) (dotted line), NPIW and NPDW (1000 m) (dashed line) and NPDW and NPBW (>3000 m) (dot-dashed line). (B) Property-property plot of VERTIGO $\delta^{15}N_{NO3}$ vs. salinity results. Conservative mixing

681 lines follow the same scheme as in (A). Since isotope ratios mix non-linearly, the conservative
682 mixing lines are curved in $\delta^{15}N$-salinity space.
683
684 Figure 5: Schematic nitrogen mass and isotope balance for station ALOHA. The upper water
685 column is divided into three vertical layers: 0-150 m, 150-300 m, and 300-500 m. Fluxes of
686 nitrate (F_{NO3}), particulate nitrogen (F_{PN}), nitrogen fixation (F_{nfix}), and remineralized organic
687 matter (F_{remin}) are reported in units of mmoles m^{-2} d^{-1}. Nitrogen isotope values for nitrate fluxes
688 ($\delta^{15}N_{NO3}$), particulate nitrogen fluxes ($\delta^{15}N_{PN}$), remineralization flux ($\delta^{15}N_{remin}$) and nitrogen
689 fixation flux ($\delta^{15}N_{Nfix}$) are reported in units of ‰ vs. AIR. Measured fluxes and isotopic values
690 are given in bold text, fluxes and isotopic values calculated from isotopic mass balances are
691 given in italics, and isotopic values calculated from isotope gradients are given in plain text.
692 Each vertical layer is solved independently for mass and isotope balance taking the sinking PN
693 fluxes and $\delta^{15}N_{PN}$ values as known and solving for fluxes of nitrate based on estimated $\delta^{15}N_{NO3}$
694 fluxes (see text). The apportionment of new nitrogen sources in the surface layer is based on an
695 assumed value for $\delta^{15}N_{Nfix}$ of 0‰ (for consistency with Dore et al., 2002) and average of
696 estimates for $\delta^{15}N_{NO3}$ flux across 150 m. Uncertainties are based on one standard deviation for
697 measured properties or propagated error based on calculated properties. The calculated fluxes
698 and isotope values are our best guesses based on the available data, and sources of uncertainty
699 are discussed in the text.
700
701 Figure 6: Depth profile of $\Delta(15,18)$ at station ALOHA. The decrease of $\Delta(15,18)$ towards the
702 surface is consistent with the introduction of nitrate with $\delta^{15}N_{NO3}$ of 0.66‰ and $\delta^{18}O_{NO3}$ of 0‰.
703

Figure 7: Property-property plot of $\delta^{15}N_{NO3}$ vs. $\delta^{18}O_{NO3}$ from station ALOHA. Error bars represent ±1 standard deviation of replicate measurements (n=2-4) for each sample. The solid arrow indicates the effect of processes that increase $\delta^{15}N_{NO3}$ and $\delta^{18}O_{NO3}$ in a 1:1 proportion (denitrification and assimilation). The dotted lines represent hypothetical extensions of the 1:1 line above and below deep $\delta^{15}N_{NO3}$ and $\delta^{18}O_{NO3}$ values. The dashed arrow represents the processes of remineralization coupled to nitrification. The decrease in $\delta^{15}N_{NO3}$ and $\delta^{18}O_{NO3}$ caused by this process between 300 m and 150 m occurs with a slope of 0.59 ± 0.03 and a y-intercept of -0.39 ± 0.14. Thus, if the $\delta^{18}O_{NO3}$ can be assumed to be close to 0‰ (see text), then the observed correlation suggests an input of nitrate with a low $\delta^{15}N$ (~0.66‰) that is consistent with nitrogen fixation.

Acknowledgements

The authors would like to acknowledge helpful discussions with John Hayes, Bill Jenkins, Dennis McGillicuddy, John Dore, Ken Buesseler, and the VERTIGO group, especially Carl Lamborg, Dave Siegel, Mary Silver, and Steve Manganini. Matthew McIlvin provided expert technical assistance. The captain and crew of the R/V Kilo Moana are also gratefully acknowledged. We also thank David Karl, Julie Granger, and two anonymous reviewers for constructive feedback on this manuscript. Support from the Woods Hole Oceanographic Institution Penzance Endowed Fund for Assistant Scientists supported KLC. Support from NSF Chemical Oceanography and Biological Oceanography programs in OCE are also gratefully acknowledged, as well as support from the Australian Commonwealth Cooperative Research Centers Program (T. T. and D. D.).

References

Abell, J., Emerson, S. and Renaud, P., 2000. Distributions of TOP, TON and TOC in the North Pacific subtropical gyre: Implications for nutrient supply in the surface ocean and remineralization in the upper thermocline. Journal of Marine Research, 58: 203-222.

Al-Mutairi, H. and Landry, M.R., 2001. Active export of carbon and nitrogen at Station ALOHA by diel migrant zooplankton. Deep-Sea Research Part II-Topical Studies in Oceanography, 48(8-9): 2083-2103.

Altabet, M.A., 1988. Variations in nitrogen isotopic composition between sinking and suspended particles: implications for nitrogen cycling and particle transformation in the open ocean. Deep Sea Research Part I, 35: 535-554.

Altabet, M.A., Deuser, W.G., Honjo, S. and Stienen, C., 1991. Seasonal and depth-related changes in the source of sinking particles in the North Atlantic. Nature, 354: 136-139.

Bishop, J.K.B., Schupack, D., Sherrell, R.M. and Conte, M.H., 1985. A Multiple Unit Large Volume in-situ Filtration System (MULVFS) for sampling oceanic particulate matter in mesoscale environments. In: A. Zirino (Editor), Mapping Strategies in Chemical Oceanography. American Chemical Society, pp. 155-175.

Böhlke, J.K., Mroczkowski, S.J. and Coplen, T.B., 2003. Oxygen isotopes in nitrate: new reference materials for O-18 : O-17 : O-16 measurements and observations on nitrate-water equilibration. Rapid Communications in Mass Spectrometry, 17(16): 1835-1846.

Brandes, J.A. and Devol, A.H., 2002. A global marine fixed nitrogen isotopic budget: Implications for Holocene nitrogen cycling. Global Biogeochemical Cycles, 16(4): 1120.

747 Brandes, J.A., Devol, A.H., Yoshinari, T., Jayakumar, D.A. and Naqvi, S.W.A., 1998. Isotopic
748 composition of nitrate in the central Arabian Sea and eastern tropical North Pacific: a
749 tracer for mixing and nitrogen cycles. Limnology and Oceanography, 43(7): 1680-1689.
750 Buesseler, K.O. et al., 2007. Revisiting carbon flux through the ocean's twilight zone. Science,
751 316(5824): 567-570.
752 Buesseler, K.O. et al., 2000. A comparison of the quantity and composition of material caught in
753 a neutrally buoyant versus surface-tethered sediment trap. Deep-Sea Research Part I-
754 Oceanographic Research Papers, 47(2): 277-294.
755 Buesseler, K.O. et al., this issue. VERTIGO (VERtical Transport In the Global Ocean): a study
756 of particle sources and flux attenuation in the North Pacific. Deep-Sea Research II, in
757 press.
758 Casciotti, K.L. and McIlvin, M.R., 2007. Isotopic analyses of nitrate and nitrite from reference
759 mixtures and application to Eastern Tropical North Pacific waters. Marine Chemistry,
760 107: 184-201.
761 Casciotti, K.L., Sigman, D.M., Galanter Hastings, M., Böhlke, J.K. and Hilkert, A., 2002.
762 Measurement of the oxygen isotopic composition of nitrate in seawater and freshwater
763 using the denitrifier method. Analytical Chemistry, 74: 4905-4912.
764 Checkley, D.M., Jr. and Miller, C.A., 1989. Nitrogen isotope fractionation by oceanic
765 zooplankton. Deep-Sea Res., 36: 1449-1456.
766 Christian, J.R., Lewis, M.R. and Karl, D.M., 1997. Vertical fluxes of carbon, nitrogen, and
767 phosphorus in the North Pacific Subtropical Gyre near Hawaii. Journal of Geophysical
768 Research, 102(C7): 15667-15677.

769 Church, M.J., Jenkins, B.D., Karl, D.M. and Zehr, J.P., 2005a. Vertical distributions of nitrogen-
770 fixing phylotypes at Stn ALOHA in the oligotrophic North Pacific Ocean. Aquatic
771 Microbial Ecology, 38(1): 3-14.
772 Church, M.J., Short, C.M., Jenkins, B.D., Karl, D.M. and Zehr, J.P., 2005b. Temporal patterns of
773 nitrogenase gene (nifH) expression in the oligotrophic North Pacific Ocean. Applied and
774 Environmental Microbiology, 71(9): 5362-5370.
775 Cline, J.D. and Kaplan, I.R., 1975. Isotopic fractionation of dissolved nitrate during
776 denitrification in the Eastern Tropical North Pacific Ocean. Marine Chemistry, 3: 271-
777 299.
778 Deutsch, C., Sarmiento, J.L., Sigman, D.M., Gruber, N. and Dunne, J.P., 2007. Spatial coupling
779 of nitrogen inputs and losses in the ocean. Nature, 445: 163-167.
780 Dore, J.E., Brum, J.R., Tupas, L.M. and Karl, D.M., 2002. Seasonal and interannual variability in
781 sources of nitrogen supporting export in the oligotrophic subtropical North Pacific Ocean.
782 Limnology and Oceanography, 47(6): 1595-1607.
783 Dore, J.E. and Karl, D.M., 1996. Nitrite distributions and dynamics at Station ALOHA. Deep-
784 Sea Research, 43: 385-402.
785 Emerson, S., Quay, P.D., Stump, C., Wilbur, D. and Schudlich, R., 1995. Chemical tracers of
786 productivity and respiration in the subtropical Pacific Ocean. Journal of Geophysical
787 Research, 100(C8): 15873-15887.
788 Falcon, L.I., Carpenter, E.J., Cipriano, F., Bergman, B. and Capone, D.G., 2004. N-2 fixation by
789 unicellular bacterioplankton from the Atlantic and Pacific oceans: Phylogeny and in situ
790 rates. Applied and Environmental Microbiology, 70(2): 765-770.

791 Fennel, K., Spitz, Y.H., Letelier, R.M., Abbott, M.R. and Karl, D.M., 2002. A deterministic
792 model for N_2 fixation at stn. ALOHA in the subtropical North Pacific Ocean. Deep-Sea
793 Research Part II-Topical Studies in Oceanography, 49(1-3): 149-174.
794 Francois, R., Altabet, M.A. and Burkle, L.H., 1992. Glacial to interglacial changes in surface
795 nitrate utilization in the Indian sector of the Southern Ocean as recorded by sediment
796 $\delta^{15}N$. Paleoceanography, 7: 589-606.
797 Granger, J., Sigman, D.M., Needoba, J.A. and Harrison, P.J., 2004. Coupled nitrogen and oxygen
798 isotope fractionation of nitrate during assimilation by cultures of marine phytoplankton.
799 Limnology and Oceanography, 49(5): 1763-1773.
800 Granger, J., Sigman, D.M., Prokopenko, M.G., Lehman, M.F. and Tortell, P.D., 2006. A method
801 for nitrite removal in nitrate N and O isotope analyses. Limnology and Oceanography:
802 Methods, 4: 205-212.
803 Karl, D. et al., 1997. The role of nitrogen fixation in biogeochemical cycling in the subtropical
804 North Pacific Ocean. Nature, 388(6642): 533-538.
805 Karl, D. et al., 2002. Dinitrogen fixation in the world's oceans. Biogeochemistry, 57/58: 47-98.
806 Karl, D.M., 1999. A sea of change: Biogeochemical variability in the North Pacific Subtropical
807 Gyre. Ecosystems, 2(3): 181-214.
808 Karl, D.M. et al., in press. The Nitrogen Cycle in the North Pacific Trades Biome: An Evolving
809 Paradigm. In: D.G. Capone, D.A. Bronk, M.R. Mulholland and E.J. Carpenter (Editors),
810 Nitrogen in the Marine Environment.
811 Karl, D.M., Bidigare, R.R. and Letelier, R.M., 2001a. Long-term changes in plankton
812 community structure and productivity in the North Pacific Subtropical Gyre: The domain

shift hypothesis. Deep-Sea Research Part II-Topical Studies in Oceanography, 48(8-9): 1449-1470.

Karl, D.M. et al., 2001b. Ecological nitrogen-to-phosphorus stoichiometry at station ALOHA. Deep-Sea Research Part II-Topical Studies in Oceanography, 48(8-9): 1529-1566.

Karl, D.M. et al., 1996. Seasonal and interannual variability in primary production and particle flux at Station ALOHA. Deep-Sea Research II, 43: 539-568.

Karl, D.M. et al., 1995. Ecosystem Changes in the North Pacific Subtropical Gyre Attributed to the 1991-92 El-Nino. Nature, 373(6511): 230-234.

Karsh, K.L., Trull, T.W., Lourey, A.J. and Sigman, D.M., 2003. Relationship of nitrogen isotope fractionation to phytoplankton size and iron availability during the Southern Ocean Iron RElease Experiment (SOIREE). Limnology and Oceanography, 48(3): 1058-1068.

Knapp, A.N., Sigman, D.M. and Lipschultz, F., 2005. N isotopic composition of dissolved organic nitrogen and nitrate at the Bermuda Atlantic time-series study site. Global Biogeochemical Cycles, 19(1).

Lamborg, C.H. et al., this issue. The Flux of Bio- and Lithogenic Material Associated with Sinking Particles in the Mesopelagic "Twilight Zone" of the Northwest and North Central Pacific Ocean. Deep-Sea Research II.

Landry, M.R., Al-Mutairi, H., Selph, K.E., Christensen, S. and Nunnery, S., 2001. Seasonal patterns of mesozooplankton abundance and biomass at Station ALOHA. Deep-Sea Research Part Ii-Topical Studies in Oceanography, 48(8-9): 2037-2061.

Lee, C., Hedges, J.I., Wakeham, S.G. and Zhu, N., 1992. Effectiveness of Various Treatments in Retarding Microbial Activity in Sediment Trap Material and Their Effects on the Collection of Swimmers. Limnology and Oceanography, 37(1): 117-130.

836 Lehmann, M.F., Bernasconi, S.M., Barbieri, A. and McKenzie, J.A., 2002. Preservation of
837 organic matter and alteration of its carbon and nitrogen isotope composition during
838 simulated and in situ early sedimentary diagenesis. Geochimica et Cosmochimica Acta,
839 66(20): 3573-3584.
840 Letelier, R.M. and Karl, D.M., 1996. Role of Trichodesmium spp in the productivity of the
841 subtropical North Pacific Ocean. Marine Ecology-Progress Series, 133(1-3): 263-273.
842 Letelier, R.M., Karl, D.M., Abbott, M.R. and Bidigare, R.R., 2004. Light driven seasonal
843 patterns of chlorophyll and nitrate in the lower euphotic zone of the North Pacific
844 Subtropical Gyre. Limnology and Oceanography, 49(2): 508-519.
845 Letelier, R.M. et al., 2000. Role of late winter mesoscale events in the biogeochemical variability
846 of the upper water column of the North Pacific Subtropical Gyre. Journal of Geophysical
847 Research-Oceans, 105(C12): 28723-28739.
848 Liu, K.-K. and Kaplan, I.R., 1989. The eastern tropical Pacific as a source of ^{15}N-enriched nitrate
849 in seawater off southern California. Limnology and Oceanography, 34: 820-830.
850 Liu, K.K., Su, M.J., Hsueh, C.R. and Gong, G.C., 1996. The nitrogen isotopic composition of
851 nitrate in the Kuroshio Water northeast of Taiwan: evidence for nitrogen fixation as a
852 source of isotopically light nitrate. Marine Chemistry, 54: 273-292.
853 Lourey, M.J., Trull, T.W., and Sigman, D.M., 2003. Sensitivity of the $\delta^{15}N$ of surface suspended
854 and deep sinking particulate organic nitrogen to Southern Ocean seasonal nitrate
855 depletion. Global Biogeochemical Cycles, 17: 1081, doi : 10.1029/2002GB001973.
856 Mahaffey, C., Benitez-Nelson, C.R., Bidigare, R.R., Rii, Y. and Karl, D.M. Nitrogen dynamics
857 within a wind-driven eddy. Deep-Sea Research II, in press.

858 Mahaffey, C., Michaels, A.F. and Capone, D.G., 2005. The conundrum of marine N_2 fixation.
859 American Journal of Science, 305: 546-595.
860 Mahaffey, C. et al., 2003. Biogeochemical signatures of nitrogen fixation in the North Atlantic.
861 Geophysical Research Letters, 30(doi: 10.1029/2002GL016542).
862 Martin, J.H., Knauer, G.A., Karl, D.M. and Broenkow, W.W., 1987. VERTEX: carbon cycling
863 in the northeast Pacific. Deep-Sea Research, 34(2): 267-285.
864 Meador, T.B., Aluwihare, L.I. and Mahaffey, C., 2007. Isotopic heterogeneity and cycling of
865 organic nitrogen in the oligotrophic ocean. Limnology and Oceanography, 52(3): 934-
866 947.
867 Minagawa, M. and Wada, E., 1986. Nitrogen isotope ratios of red tide organisms in the East
868 China Sea: A characterization of biological nitrogen fixation. Marine Chemistry, 19: 245-
869 249.
870 Montoya, J.P., Carpenter, E. and Capone, D., 2002. Nitrogen fixation and nitrogen isotope
871 abundance in zooplankton of the oligotrophic North Atlantic. Limnology and
872 Oceanography, 47: 1617-1628.
873 Montoya, J.P. et al., 2004. High rates of N-2 fixation by unicellular diazotrophs in the
874 oligotrophic Pacific Ocean. Nature, 430(7003): 1027-1031.
875 Sabine, C.L., Mackenzie, F.T., Winn, C.D. and Karl, D.M., 1995. Geochemistry of carbon
876 dioxide in seawater at the Hawaii Ocean Time series station ALOHA. Global
877 Biogeochemical Cycles, 9(4): 637-651.
878 Sakamoto, C.M. et al., 2004. Influence of Rossby waves on nutrient dynamics and the plankton
879 community structure in the North Pacific subtropical gyre. Journal of Geophysical
880 Research, 109(doi:10.1029/2003JC001976).

881 Scharek, R., Latasa, M., Karl, D.M. and Bidigare, R.R., 1999. Temporal variations in diatom
882 abundance and downward vertical flux in the oligotrophic North Pacific gyre. Deep-Sea
883 Research Part I-Oceanographic Research Papers, 46(6): 1051-1075.
884 Sigman, D.M., Altabet, M.A., Francois, R., McCorkle, D.C. and Fischer, G., 1999. The $\delta^{15}N$ of
885 nitrate in the Southern Ocean: Consumption of nitrate in surface waters. Global
886 Biogeochemical Cycles, 13(4): 1149-1166.
887 Sigman, D.M. et al., 2001. A bacterial method for the nitrogen isotopic analysis of nitrate in
888 seawater and freshwater. Analytical Chemistry, 73(17): 4145-4153.
889 Sigman, D.M. et al., 2005. Coupled nitrogen and oxygen isotope measurements of nitrate along
890 the eastern North Pacific margin. Global Biogeochemical Cycles, 19(4): GB4022.
891 Steinberg, D.K., Cope, J.S., Wilson, S.E. and Kobari, T., this issue. A comparison of
892 mesopelagic zooplankton community structure in the subtropical and subarctic Pacific
893 Ocean. Deep-Sea Research II, in press.
894 Sutka, R.L., Ostrom, N.E., Ostrom, P.H. and Phanikumar, M.S., 2004. Stable nitrogen isotope
895 dynamics of dissolved nitrate in a transect from the North Pacific Subtropical Gyre to the
896 Eastern Tropical North Pacific. Geochimica et Cosmochimica Acta, 68(3): 517-527.
897 Talley, L.D., 1985. Ventilation of the subtropical North Pacific: The shallow salinity minimum.
898 Journal of Physical Oceanography, 15: 633-649.
899 Talley, L.D., 1993. Distribution and Formation of North Pacific Intermediate Water. Journal of
900 Physical Oceanography, 23: 517-537.
901 Trull, T.W., Davies, D., and Casciotti, K.L., 2008. Insights into nutrient assimilation and export
902 in naturally iron-fertilized waters of the Southern Ocean from nitrogen, carbon, and
903 oxygen isotopes. Deep-Sea Research II, in press.

904 Vaillancourt, R.D., Marra, J., Seki, M.P., Parsons, M.L. and Bidigare, R.R., 2003. Impact of a
905 cyclonic eddy on phytoplankton community structure and photosynthetic competency in
906 the subtropical North Pacific Ocean. Deep-Sea Research I, 50: 829-847.
907 Valdes, J.R. and Price, J.F., 2000. A neutrally buoyant, upper ocean sediment trap. Journal of
908 Atmospheric and Oceanic Technology, 17(1): 62-68.
909 Villareal, T.A., Altabet, M.A. and CulverRymsza, K., 1993. Nitrogen Transport by Vertically
910 Migrating Diatom Mats in the North Pacific-Ocean. Nature, 363(6431): 709-712.
911 Villareal, T.A., Woods, S., Moore, J.K. and CulverRymsza, K., 1996. Vertical migration of
912 rhizosolenia mats and their significance to NO_3^- fluxes in the central north Pacific gyre.
913 Journal of Plankton Research, 18(7): 1103-1121.
914 Voss, M., Dippner, J.W. and Montoya, J.P., 2001. Nitrogen isotope patterns in the oxygen-
915 deficient waters of the Eastern Tropical North Pacific Ocean. Deep-Sea Research Part I-
916 Oceanographic Research Papers, 48(8): 1905-1921.
917 Wada, E. and Hattori, A., 1990. Nitrogen in the Sea: Forms, Abundances and Rate Processes.
918 CRC Press, Boca Raton, FL.
919 Wankel, S.D., Kendall, C., Pennington, J.T., Chavez, F.P. and Paytan, A., 2007. Nitrification in
920 the euphotic zone as evidenced by nitrate dual isotopic composition: Observations from
921 Monterey Bay, California. Global Biogeochemical Cycles, 21(2): GB2009.
922 Zehr, J.P., Mellon, M.T. and Zani, S., 1998. New nitrogen-fixing microorganisms detected in
923 oligotrophic oceans by amplification of nitrogenase (nifH) genes. Applied and
924 Environmental Microbiology, 6: 3444-3450.
925 Zehr, J.P. et al., 2001. Unicellular cyanobacteria fix N-2 in the subtropical North Pacific Ocean.
926 Nature, 412(6847): 635-638.

Figure 1

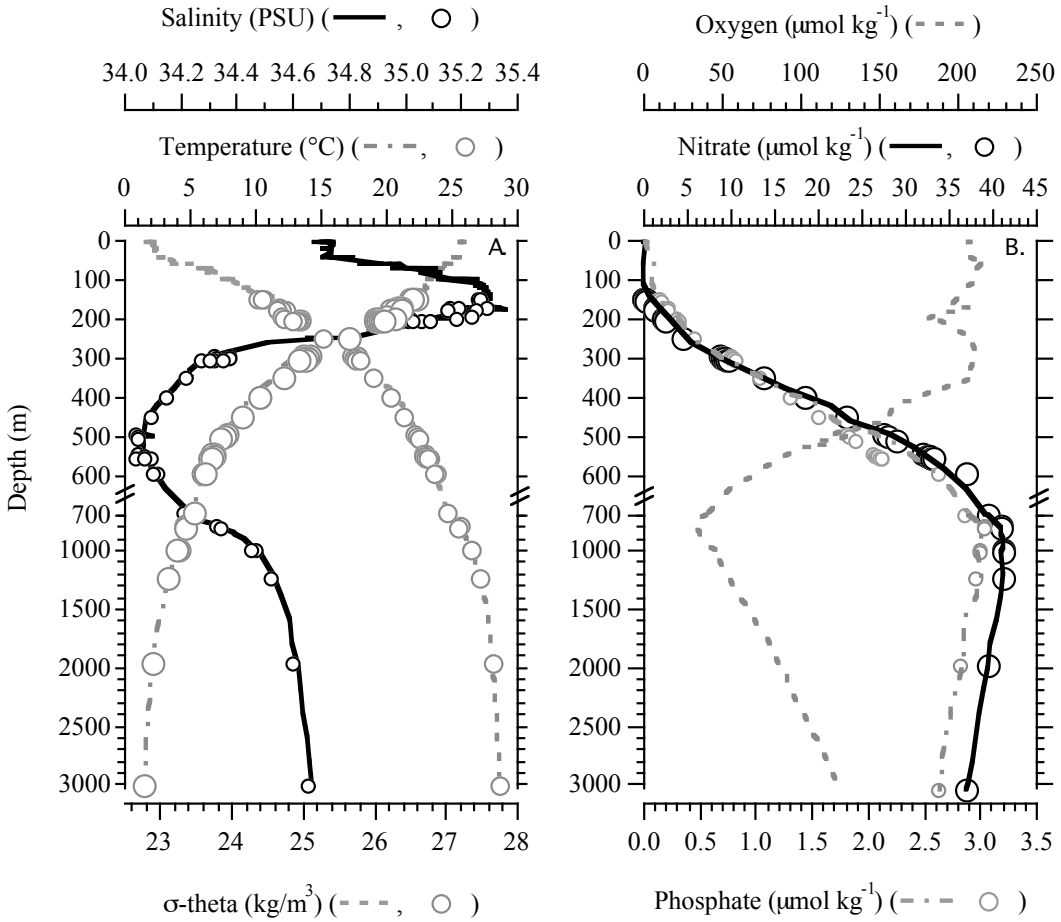
Salinity (PSU) (,)
34.0 34.2 34.4 34.6 34.8 35.0 35.2 35.4
Temperature (°C) (,)
0 5 10 15 20 25 30
Depth (m)
0 100 200 300 400 500 600 700 1000 1500 2000 2500 3000
A.
23 24 25 26 27 28
σ-theta (kg/m3) (,)
Oxygen (µmol kg-1) ( )
0 50 100 150 200 250
Nitrate (µmol kg-1) (,)
0 5 10 15 20 25 30 35 40 45
B.
0.0 0.5 1.0 1.5 2.0 2.5 3.0 3.5
Phosphate (µmol kg-1) ( )

Figure 2

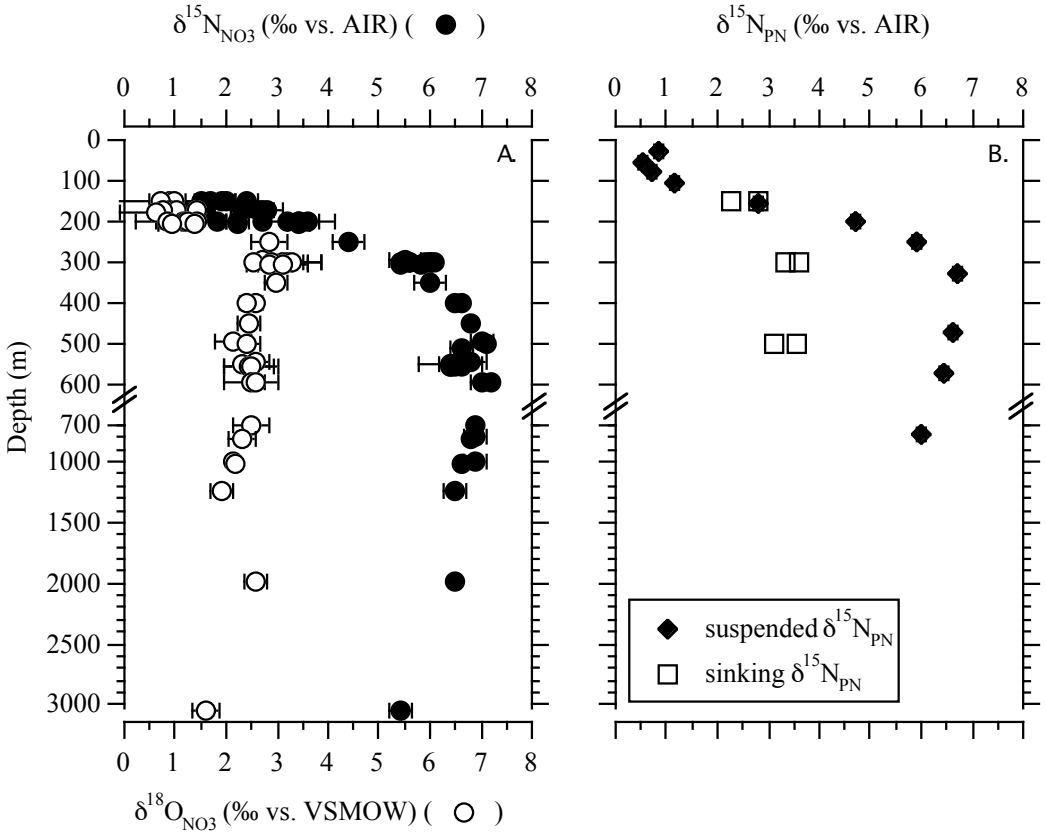
δ15NNO3 (‰ vs. AIR) (●)
δ15NPN (‰ vs. AIR)
A.
B.
Depth (m)
0
100
200
300
400
500
600
700
1000
1500
2000
2500
3000
0 1 2 3 4 5 6 7 8
suspended δ15NPN
sinking δ15NPN
δ18ONO3 (‰ vs. VSMOW) (○)

Figure 3

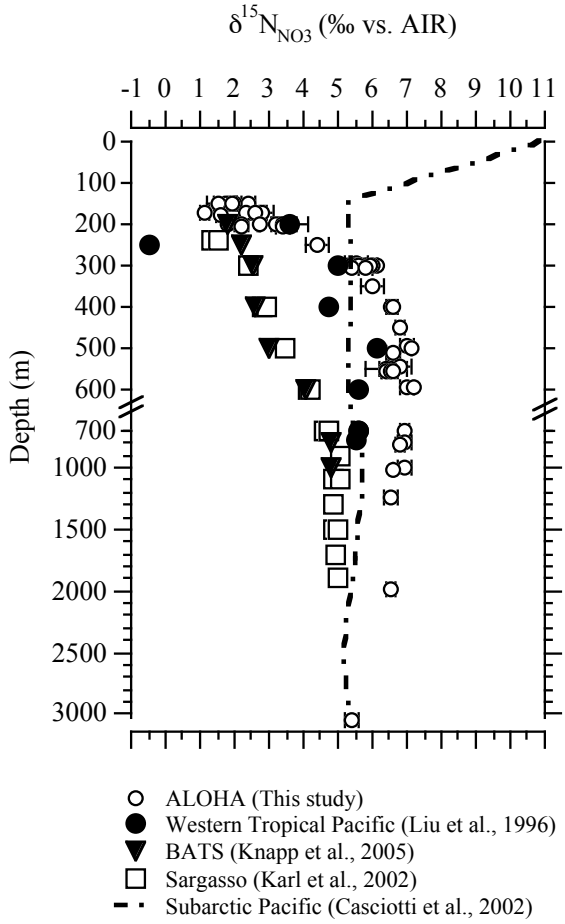
δ15NNO3 (‰ vs. AIR)
-1 0 1 2 3 4 5 6 7 8 9 10 11
Depth (m)
0
100
200
300
400
500
600
700
1000
1500
2000
2500
3000
ALOHA (This study)
Western Tropical Pacific (Liu et al., 1996)
BATS (Knapp et al., 2005)
Sargasso (Karl et al., 2002)
Subarctic Pacific (Casciotti et al., 2002)

Figure 4

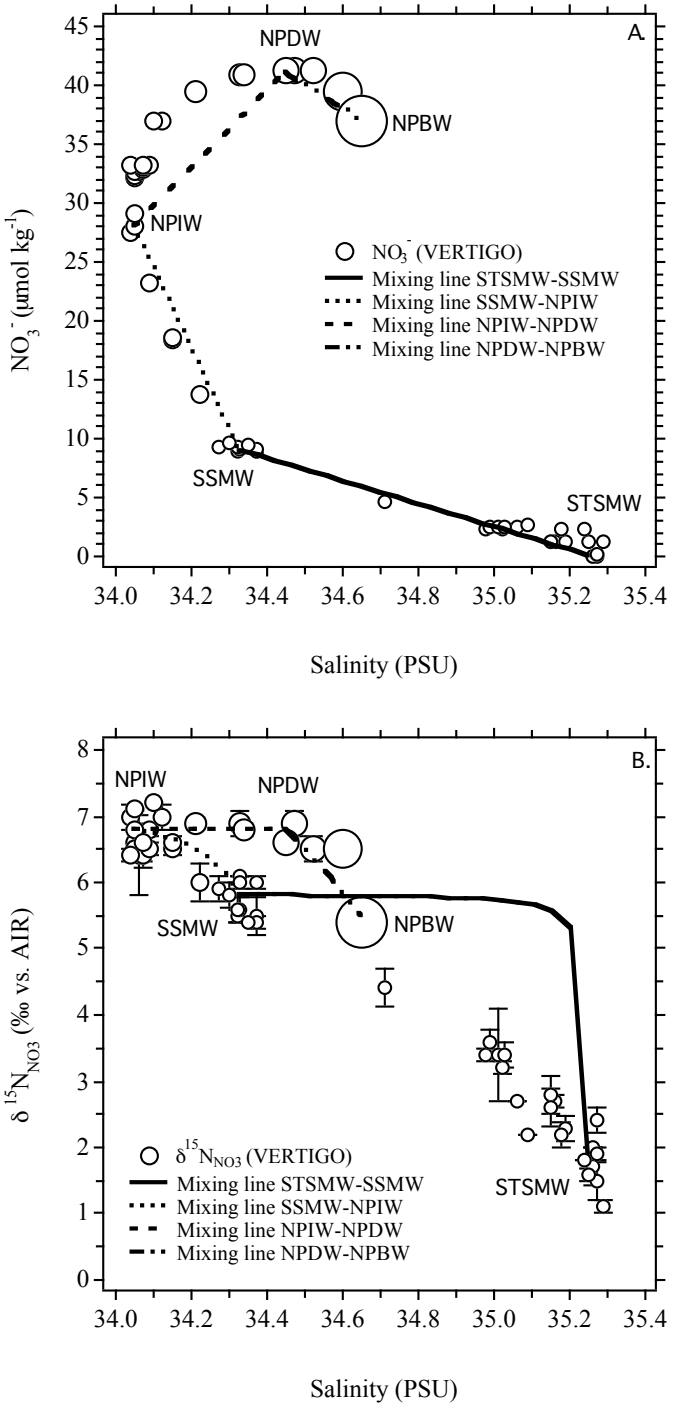
A.
NPDW
NPBW
NPIW
SSMW
STSMW
NO_3^- (VERTIGO)
Mixing line STSMW-SSMW
Mixing line SSMW-NPIW
Mixing line NPIW-NPDW
Mixing line NPDW-NPBW
NO_3^- (µmol kg^{-1})
Salinity (PSU)
B.
NPIW
NPDW
SSMW
NPBW
STSMW
$\delta^{15}N_{NO3}$ (VERTIGO)
Mixing line STSMW-SSMW
Mixing line SSMW-NPIW
Mixing line NPIW-NPDW
Mixing line NPDW-NPBW
$\delta^{15}N_{NO3}$ (‰ vs. AIR)
Salinity (PSU)

Figure 5

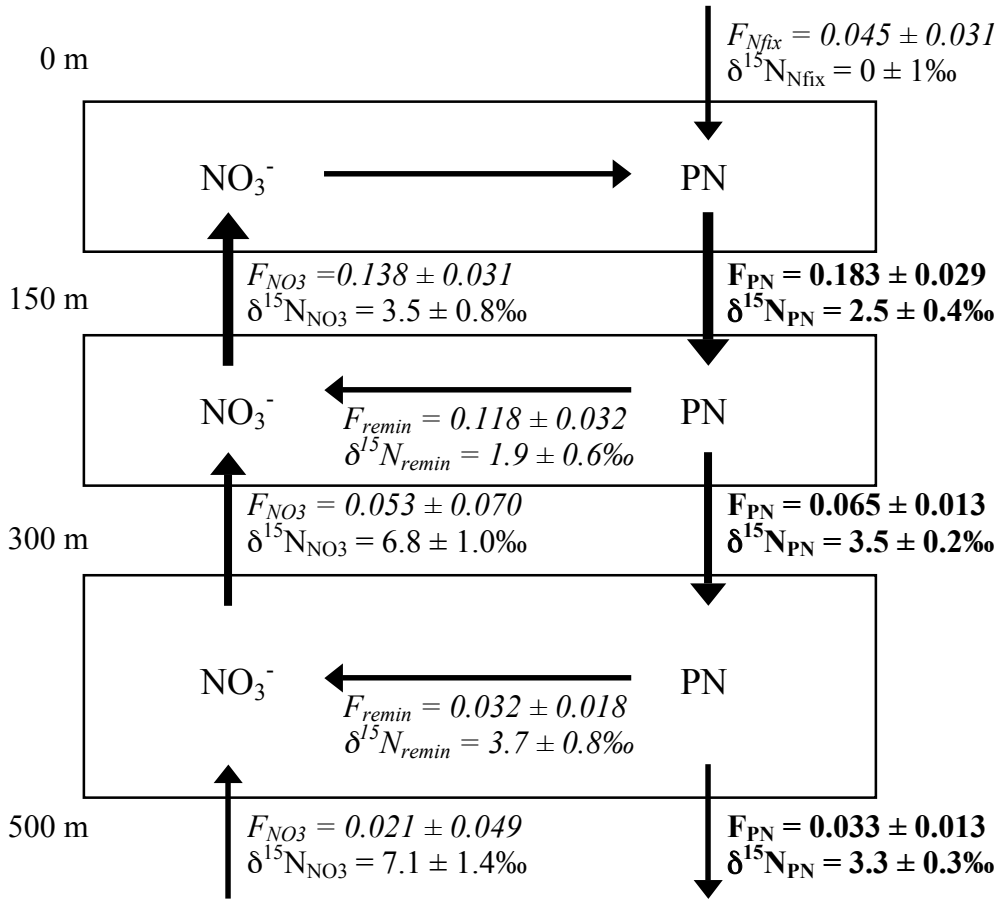
0 m
F_{Nfix} = 0.045 ± 0.031
$\delta^{15}N_{Nfix}$ = 0 ± 1‰
NO_3^-
PN
150 m
F_{NO3} =0.138 ± 0.031
$\delta^{15}N_{NO3}$ = 3.5 ± 0.8‰
F_{PN} = 0.183 ± 0.029
$\delta^{15}N_{PN}$ = 2.5 ± 0.4‰
NO_3^-
F_{remin} = 0.118 ± 0.032
$\delta^{15}N_{remin}$ = 1.9 ± 0.6‰
PN
300 m
F_{NO3} = 0.053 ± 0.070
$\delta^{15}N_{NO3}$ = 6.8 ± 1.0‰
F_{PN} = 0.065 ± 0.013
$\delta^{15}N_{PN}$ = 3.5 ± 0.2‰
NO_3^-
F_{remin} = 0.032 ± 0.018
$\delta^{15}N_{remin}$ = 3.7 ± 0.8‰
PN
500 m
F_{NO3} = 0.021 ± 0.049
$\delta^{15}N_{NO3}$ = 7.1 ± 1.4‰
F_{PN} = 0.033 ± 0.013
$\delta^{15}N_{PN}$ = 3.3 ± 0.3‰

Figure 6

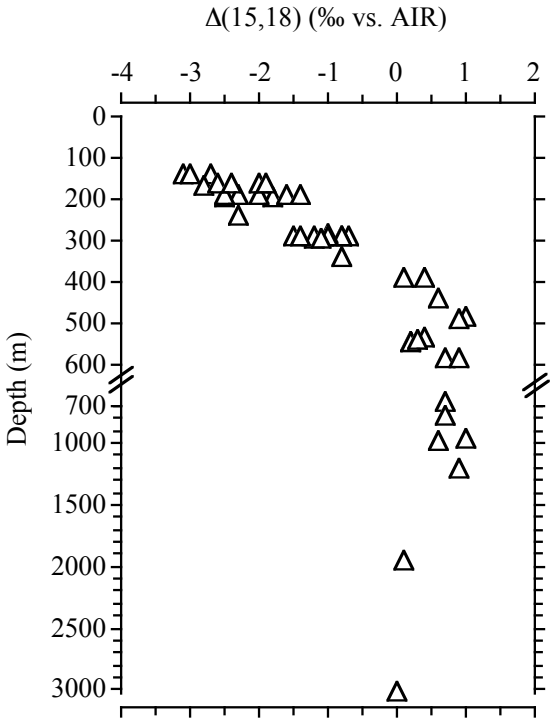
Δ(15,18) (‰ vs. AIR)
-4
-3
-2
-1
0
1
2
Depth (m)
0
100
200
300
400
500
600
700
1000
1500
2000
2500
3000

Figure 7